following conclusions or observations. All the evidence points to $W(t\text{-}Bu_2Me_2dsp)_2$ complexes that contain $t\text{-}Bu_2Me_2dsp^{2-}$ ligands chelating in a nonplanar fashion. To have a $W(t\text{-}Bu_2Me_2dsp)_2$ complex with no apparent symmetry requires that one and probably both $t\text{-}Bu_2Me_2dsp^{2-}$ ligands are bonding in a nonplanar mode. How different the modes of wrapping vary from one complex to the next is difficult to assert. That the R_f values for the four complexes range from 0.92 to 0.29 suggests the backbone of the $t\text{-}Bu_2Me_2dsp^{2-}$ ligands are oriented in quite different ways from one complex to the next.

In spite of the uniqueness of the ^1H NMR spectrum of each $W(t\text{-}Bu_2Me_2dsp)_2$ complex, the electronic spectra of the four $W(t\text{-}Bu_2Me_2dsp)_2$ complexes are nearly superimposable on one another. This suggests that the four nitrogen donor atoms and the four oxygen donor atoms may occupy similar sites in all four complexes. It is probable that the WN_4O_4 chromophore is similar in each complex but that the orientation of the remainder of the $t\text{-}Bu_2Me_2dsp^{2-}$ ligands are skewed in a different fashion in each complex.

We find no special significance in the number of isomers isolated. In fact, there may be still other $W(t\text{-}Bu_2Me_2dsp)_2$ complexes present in the product mixture that were overlooked. The large number of isomers isolated, along with the nature of the ^1H NMR spectra obtained for the $W(t\text{-}Bu_2Me_2dsp)_2$ complexes would appear to rule out a dodecahedral complex containing $t\text{-}Bu_2Me_2dsp^{2-}$ ligands spanning the *mam* edges as was found for the $Zr(dsp)_2$ complex. This stereochemistry is clearly favorable from the standpoint of steric considerations. That this stereochemistry appears not to be observed for the $W(t\text{-}Bu_2Me_2dsp)_2$ complex indicates that electronic effects are at least partially at play in determining the ultimate stereochemistry of the $W(t\text{-}Bu_2Me_2dsp)_2$ complexes.

Another piece of evidence that suggests that the $t\text{-}Bu_2Me_2dsp^{2-}$ ligand is not spanning the *mam* edges in the $W(t\text{-}Bu_2Me_2dsp)_2$ complexes is the results obtained from mixed-ligand studies. Our attempts to synthesize a mixed-ligand eight-coordinate complex containing the $t\text{-}Bu_2Me_2dsp^{2-}$ ligand and the bidentate ligand $mpic^-$, where $mpic^-$ = 5-methylpicolinato, have failed.[31] The $mpic^-$ ligand is believed to span the four *m* edges of the dodecahedron, with the nitrogen donors occupying the B sites and the oxygen donors occupying the A sites in the eight-coordinate complex tetrakis(5-methylpicolinato)tungsten(IV), $W(mpic)_4$.[15b] Assuming this is the case and assuming that the $t\text{-}Bu_2Me_2dsp^{2-}$ ligand could span the *mam* edges, the $W(t\text{-}Bu_2Me_2dsp)(mpic)_2$ complex should exist. Since it does not, we conclude that two ligands are incompatible and that the $t\text{-}Bu_2Me_2dsp^{2-}$ ligand will not span the *mam* edges when forming an eight-coordinate tungsten(IV) complex.

Acknowledgment. Support of this work by the Horace H. Rackham School of Graduate Studies of the University of Michigan is gratefully acknowledged.

Registry No. 1b, 94706-50-0; $W(t\text{-}Bu_2Me_2dsp)_2$, 94706-51-1; tungsten hexacarbonyl, 14040-11-0; trimethylamine–borane, 75-22-9; 4,5-dimethyl-*o*-phenylenediamine, 3171-45-7; 5-*tert*-butyl-2-hydroxybenzaldehyde, 2725-53-3.

(31) Unpublished results.
(32) The group notation is being changed in accord with recent actions by IUPAC and ACS nomenclature committees. A and B notation is being eliminated because of wide confusion. Group I becomes groups 1 and 11, group II becomes groups 2 and 12, group III becomes groups 3 and 13, etc.

Contribution from the Departments of Chemistry and Biochemistry, Louisiana State University, Baton Rouge, Louisiana 70803-1804, and Perkin-Elmer Corporation, Norwalk, Connecticut 06856

Square-Planar Cis- and Trans-C–Palladium(II) Complexes of N-Electron-Deficient Heteroaromatic Ligands.[1] Ligand Synthesis, Complexation, Spectral Analyses, and Complex Interaction with Phage PM2 DNA[+]

GEORGE R. NEWKOME,*[†] WALLACE E. PUCKETT,[†] GARRY E. KIEFER,[†] VINOD K. GUPTA,[†] FRANK R. FRONCZEK,[†] DANIEL C. PANTALEO,[†,2] GREGORY L. McCLURE,[‡] JANELL B. SIMPSON,[§] and WALTER A. DEUTSCH[§]

Received August 22, 1984

A new class of organometallic Pd(II) complexes has been synthesized utilizing functionalized bipyridine or phenanthroline ligands that are capable of forming intramolecular cis bis anionic carbon to metal bonds. The ^1H and ^{13}C NMR spectra for the ligands and related complexes are reported. The tetradentate bipyridine ligand undergoes facile complexation with Pd(II) salts to give the complex possessing two C–Pd bonds, whereas the corresponding phenanthroline analogue is capable of forming only a single C–Pd bond. Single-crystal X-ray structure analyses have revealed that angular distortions are responsible for these reactivity differences. ^{13}C NMR and IR spectra of these complexes and the related pyridine and pyrazine complexes having trans-C–metal bonds are also presented. Details of the spectral assignments are given, and the ^{13}C NMR chemical shifts are interpreted in terms of the strain and/or electronic effects. The stereochemistry of the chelate ring was found to be the most important factor in determining the chemical shifts. The binding of *cis*-organopalladium complexes to phage PM2 DNA is reported where increased binding is correlated with the presence of cis-C–Pd bonds.

Introduction

There has been considerable attention focused on the study of palladium complexes in organic synthesis,[3] catalytic processes,[4] chemical reactivity,[5,6] spectroscopy,[7,8] and structural aspects.[9] Recently, new classes of stable organopalladium(II) complexes, which possess both intramolecular C- and N-coordination,[10-12] have been prepared. The increasing importance of such cycloorganometallic complexes has led us to investigate cyclic complexes

[†] Department of Chemistry, Louisiana State University.
[‡] Perkin-Elmer Corp.
[§] Department of Biochemistry, Louisiana State University.

(1) Chemistry of Heterocyclic Compounds Series. 94. Part 92: Newkome, G. R.; Gupta, V. K.; Fronczek, F. R.; Pappalardo, S. *Inorg. Chem.* **1984**, *23*, 2400.
(2) On leave from Bloomsburg State College, Bloomsburg, PA (1980).
(3) Holton, R. A. *J. Am. Chem. Soc.* **1977**, *99*, 8083.
(4) Maitlis, P. M. "The Organic Chemistry of Palladium"; Academic Press: New York, 1971.
(5) Bahsoun, A.; Dehand, J.; Pfeffer, M.; Zinsius, M.; Bouaoud, S. E.; Le Borgne, G. *J. Chem. Soc., Dalton Trans.* **1979**, 547.

0020-1669/85/1324-0811$01.50/0

with enhanced chemical and thermal stability, from which detailed spectroscopic and structural correlations could be readily deduced.

At the onset of our work in this area, numerous metallacycles had been prepared by initial generation of a metal–heteroatom bond, followed by ortho-C(sp^2) coordination with an aromatic ring via either transmetalation or direct C–H bond insertion.[13] The *n*-membered (*n* is usually 5) chelate ring purportedly imparts an inherent stability to the resultant C(sp^2)–metal bond:[14]

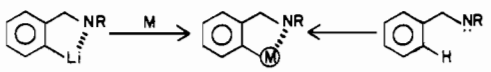

Relatively few stable metallacycles with metal–C(sp^3) bonds had been reported prior to 1980, of which these limited examples with acyclic metal–C(sp^3) bonds, such as Pt(II) complexes of acetylacetone and ethyl acetoacetate, were shown to possess an unusually high degree of overall stability.[15] Further, certain O-bonded acetylacetone (acac) complexes were isomerized to the C-bonded species;[14,15] the metal–C(sp^3) bond stability was attributed to the electron-withdrawing character of the adjacent β-dicarbonyl groups.

Incorporation of the salient stabilizing factors (five-membered ring, directed N-donor, and an available acidic hydrogen) into a single ligand generated the trans model **1**.[16] The related cis-

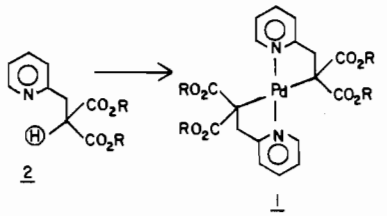

2 **1**

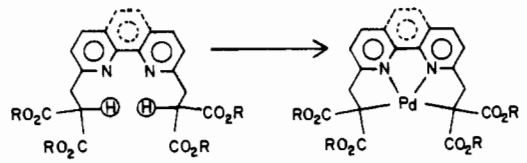

13

tetradentate ligand **13** would then utilize bis N-donors, such as either bipyridine or phenanthroline, and appropriate β-dicarbonyl units connected by a single methylene group.

In addition to ligand syntheses and subsequent complexation, these organometallics offered several other interesting features: (1) development of new preparative procedures for forming the stable metal–ligand bonds, (2) insight into the chemical reactivity of these metal–carbon bonds, and (3) correlation of the spectral and structural data. Also the pronounced DNA activity,[17] noted in our preliminary communication for the cis complexes (e.g. **13**),

Scheme I

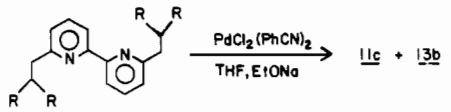

11c + **13b**

as well as their homo- and heterogenous catalytic activity[18] adds further impetus. Thus, we herein offer a systematic ^{13}C NMR study of numerous diamagnetic square-planar palladium(II) complexes derived from pyridine, pyrazine, bipyridine, and phenanthroline. The detailed single-crystal X-ray studies on twelve of these complexes herein reported were conducted to provide additional support to the electronic and conformational subtleties, which could influence the spectroscopic data.

The ^{13}C chemical shifts in the complexes are dependent on three major terms: diamagnetic shielding, paramagnetic shielding, and an anisotropic term, of which the paramagnetic term contributes most significantly to the observed chemical shift.[19] ^{13}C NMR data are of particular interest in organometallics because of their noted defiance of substituent additivity rules,[20] which have been so well documented for many series of organic molecules. Some researchers have proposed that a metal d-orbital nonbonded shielding term may contribute substantially to the normal bonding interactions, as reflected by the chemical shifts.[21] This term is sensitive to the metal–ligating-atom distance and may be responsible for the inconsistency in additivity factors. In view of these conjectures, we will herein consider the ^{13}C chemical shift data via the "*strain effect*" instilled by the subtle structural changes within the microenvironment of the cyclometalated rings of a closely related series of Pd(II)–C(sp^3) complexes.

The electron density of the Pd(II) ion may introduce an important "*electronic effect*" on the chelate ring carbon atoms as well as N-donor ligand. The ^{13}C chemical shifts are thus interpreted in terms of the strain and/or electronic effects. Since the absolute ^{13}C chemical shifts are dependent on numerous factors and can vary considerably with diverse ligands, we have elected to use the ligand to complex ^{13}C chemical shift difference [$\Delta\delta$-(^{13}C)] as a reasonable measure of structural and electronic variations upon complexation.

The infrared spectra of the complexes have also been incorporated to characterize, as fully as possible, the change in the electronic environment upon Pd(II)–C(sp^3) bond formation.

Results

I. Synthesis of Ligands. The preparation of the ligands was accomplished by treatment of the appropriate, freshly purified halomethyl derivative[22,23] with the alkyl malonate in the presence of anhydrous K_2CO_3 in pure[24] *N,N*-dimethylformamide (DMF):

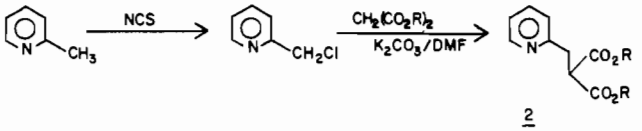

2

Generally, one major 2-substituted malonate product was isolated in greater than 90% yield. Other more classical approaches using either ether or alcoholic solvents with either alkali hydride or

(6) Mantovani, A.; Crociani, B. *J. Organomet. Chem.* **1982**, *236*, C37.
(7) Matsubayashi, G.; Kondo, Y. *J. Organomet. Chem.* **1981**, *219*, 269.
(8) Cocivera, M.; McAlees, A. J.; McCrindle, R.; Szezecinski, P. *J. Organomet. Chem.* **1982**, *235*, 97.
(9) Schwarzenbach, D.; Pinkerton, A.; Chapius, G.; Wenger, J.; Ros, R.; Roulet, R. *Inorg. Chim. Acta* **1977**, *25*, 255.
(10) Dehand, J.; Pfeffer, M. *Coord. Chem. Rev.* **1976**, *18*, 327.
(11) Bruce, M. I. *Angew. Chem., Int. Ed. Engl.* **1977**, *16*, 73.
(12) Omae, I. *Chem. Rev.* **1979**, *79*, 287.
(13) Stout, D. M.; Meyers, A. I. *Chem. Rev.* **1982**, *82*, 223.
(14) (a) Ito, T.; Kiriyoma, T.; Nakamura, Y.; Yamamoto, A. *Bull. Chem. Soc. Jpn.* **1976**, *49*, 3257. (b) Okeya, S.; Kawaguchi, S. *Inorg.* Chem. **1977**, *16*, 1730. (c) Vanchessan, S.; Kurisacose, J. C. *J. Sci. Ind. Res.* **1983**, *42*, 132.
(15) (a) Yamada, K.; Baba, S.; Nakamura, Y.; Kawaguchi, S. *Bull. Chem. Soc. Jpn.* **1983**, *56*, 1383. (b) Ito, T.; Yamamoto, A. *J. Organomet. Chem.* **1979**, *174*, 237.
(16) Newkome, G. R.; Gupta, V. K.; Fronczek, F. R. *Organometallics* **1982**, *1*, 907; **1983**, *2*, 785.
(17) (a) Deutsch, W. A.; Spiering, A. L.; Newkome, G. R. *Biochem. Biophys. Res. Commun.* **1980**, *97*, 1220.
(18) (a) Newkome, G. R.; Yoneda, A. *Makromol. Chem., Rapid Commun.*, in press. (b) Newkome, G. R.; Gupta, V. K. submitted for publication in *Makromol. Chem., Rapid Commun.*
(19) Levy, G. C.; Nelson, G. L. "Carbon-13 Nuclear Magnetic Resonance for Organic Chemists"; Wiley-Interscience: New York, 1972.
(20) Mann, B. E.; Taylor, B. F. "^{13}C NMR Data for Organometallic Compounds"; Academic Press: New York, 1981.
(21) Cooper, D. G.; Hughes, R. P.; Powell, J. *J. Am. Chem. Soc.* **1972**, *94*, 9244.
(22) Newkome, G. R.; Puckett, W. E.; Kiefer, G. E.; Gupta, V. K.; Xia, Y.; Coreil, M.; Hackney, M. A. *J. Org. Chem.* **1982**, *47*, 4116.
(23) Newkome, G. R.; Kiefer, G. E.; Xia, Y.-J.; Gupta, V. K. *Synthesis* **1984**, 676.
(24) (a) Newkome, G. R.; Robinson, J. M. *Tetrahedron Lett.* **1974**, 691. (b) Trisler, J. C.; Freasier, B. F.; Wu, S.-M. *Tetrahedron Lett.* **1974**, 687.

Scheme II

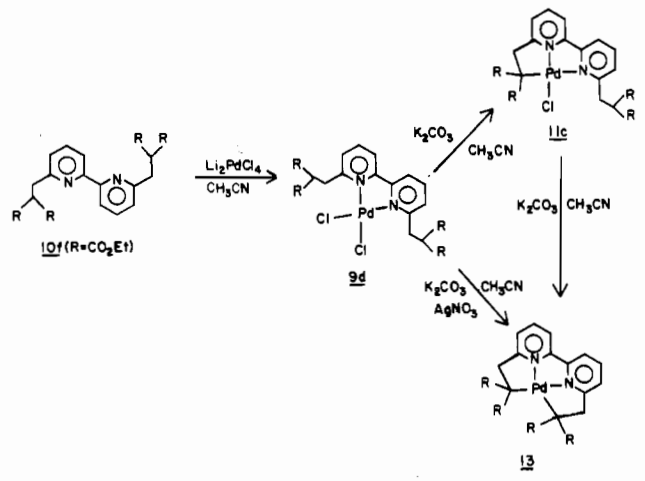

alkoxide bases gave reasonable (50–70%) yields but were more cumbersome and offered no special advantages over the K_2CO_3/DMF procedure.

Over the years the original lengthy routes (A,[25] ArBr → ArCHO → $ArCH_2OH$ → $ArCH_2X$; B,[22] $ArCH_3$ → $ArCH_2OAc$ → $ArCH_2OH$ → $ArCH_2X$) have been replaced by the simple free-radical chlorination of the desired heteroaryl methyl group under specialized conditions.[23] It should be noted that *extreme care* must be taken in view of the potential alkylating properties—common with all of these halomethyl starting materials. The simplest member of this series—2-(chloromethyl)-pyridine hydrochloride—has been shown to be *toxic* but not yet a carcinogen.[26]

II. Synthesis of Palladium(II)-C(sp^3) Complexes. Complexation was conducted initially by the procedure illustrated in Scheme I. This obvious route was eventually abandoned since the inherent problems [e.g. (1) competitive reduction of $PdCl_2$ to Pd(0), (2) reasonable but generally low product yield, and (3) the undesirable presence of benzonitrile] could not be circumvented. The procedure shown in Scheme II has been developed as a general, efficient route to these organometallics. Formation of the Pd–C bond is extremely sensitive to the reaction conditions but does occur smoothly when (1) initial formation of the N–Pd bond is conducted in a homogeneous environment and (2) the intermediate carbanion(s) is (are) generated at 25 °C via the K_2CO_3/CH_3CN procedure. This method offers several advantages: (1) there is little or no Pd(II) reduction, (2) the trace byproducts are easily removed, and (3) the yields are generally greater than 80%.

The generation of **7** from **8** upon treatment with Li_2PdCl_4 and K_2CO_3 occurred without adding $AgNO_3$. The formation of **11** or **13** can, however, be controlled by the addition of $AgNO_3$, except in the case of the carbomethoxy analogue, from which only **13a** was isolated with or without added $AgNO_3$. With the more bulky alkyl esters, only the monometalated intermediates were isolated without the presence of $AgNO_3$; subsequent addition of silver ion rapidly transformed the monochloro intermediates to the bismetalated products. It is generally better to isolate the monometalated intermediate and then subject it to these cyclization conditions, since purification in each step is facile and high yield. The phenanthrolines **15** were converted only to the monometalated species **17**, and even under diverse reaction conditions the formation of the second Pd–C bond was never realized. This failure of **17** to cyclize was due to the enhanced rigidity imposed by the phenanthroline backbone, thus increasing the ligand bite.

These complexes are unique for several reasons: (1) They possess one or two C(sp^3)–Pd σ bonds; (2) the bismetalated products (e.g., **13**) have a novel 5.5.5-tricyclic ring system circumscribed by a rigid tetradentate framework;[27] (3) little or no

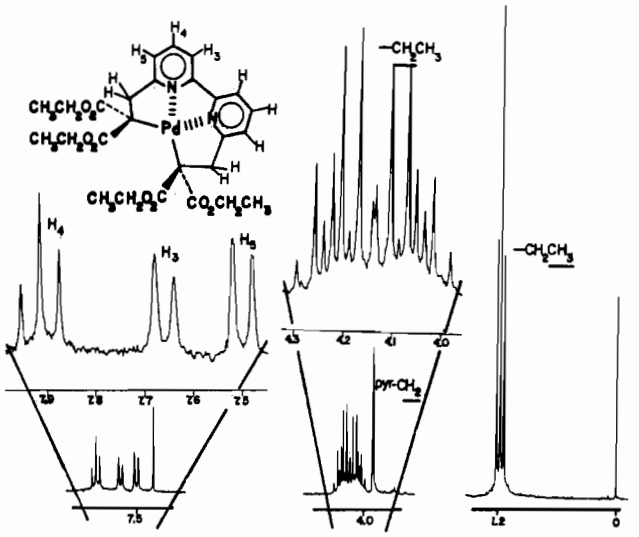

Figure 1. 200-MHz ^1H NMR spectrum of **13b** in $CDCl_3$ with expanded aromatic and ester methylene regions.

Scheme III

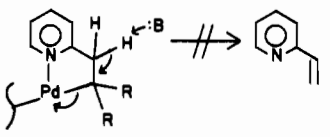

degradation by air, light, or dissolution is noted. In solution (C_6H_6, CH_2Cl_2, EtOAc, and most alcohols), the complexes are stable indefinitely. The wide range of solubilities is noteworthy; however, appreciable decomposition in $CHCl_3$ occurs, presumably due to traces of HCl. The bis complexes **13** undergo a visible chromophoric change upon addition of traces of water to an alcohol solution; however, in vacuo removal of the solvent restores the original chromophore. (4) These organometallics are among the first stable C–Pd species containing an acidic, abstractable β-hydrogen.[28,29] Degradation to the olefin was never observed (Scheme III); presumably the appropriate orbital alignment cannot be realized in the five-membered chelate ring.

Despite their enhanced stability, the bis-cis complexes **13** are reactive, albeit marginally, with electrophile–nucleophile pairs or dipolarophiles. Attempted recrystallization of **13b** from benzene with traces of AcOH afforded **11d** via slow C–Pd bond cleavage. Such fragmentation is quite predictable and precedented.[30] Further, the following ^{13}C NMR data substantiate an increased electron density on the methine carbon upon complexation.

The most striking feature in the ^1H NMR spectrum (Figure 1) of **13b** is the symmetrical 16-line pattern for the ester methylene hydrogens indicative of a magnetically different environment for these hydrogens. There are, however, neither neighboring chiral centers nor any appreciable bond-rotational barriers, but there does exist a distorted coordination around the metal. This overall molecular distortion leads to the molecular dissymmetry, the

(25) Newkome, G. R.; Kohli, D. K.; Fronczek, F. *J. Chem. Soc., Chem. Commun.* **1980**, 9.
(26) Bailey, T. D., personal communication, Reilly Tar and Chemical Corp.

(27) In the course of di-ortho-metalation studies, *N,N'*-dimethyl-*N,N'*-bis-(*o*-bromobenzyl)ethylenediamine with anhydrous iron(II) chloride gave a distorted-tetrahedral 5.5.5-fused ring system containing a pivotal ferrous iron. However, when $PhCH_2(Me)N(CH_2)_nN(Me)CH_2Ph$ (n = 2 or 3) was treated with Na_2PdCl_4 (or Na_2PtCl_4), the intermediate bidentate bis-N complex underwent internal cyclometalation to give a mono-ortho-metalated compound; only when n = 3 does bis-ortho-metalation occur (i.e., to form the 5.6.5-fused ring system). The distorted-square-planar 5.5.5 product (for n = 2) could not be prepared, as explained on steric grounds. In stark contrast to these results, the literature abounds in 5.5.5 complexes derived from nitrogen, oxygen, and/or sulfur donor ligands: Kupper, F. W. *J. Organomet. Chem.* **1968**, *13*, 219.
(28) Stille, J. K.; Lau, K. S. Y. *J. Am. Chem. Soc.* **1976**, *98*, 5841.
(29) (a) Hayashi, T.; Hegedus, L. S. *J. Am. Chem. Soc.* **1977**, *99*, 7093. (b) Heck, R. F. *Pure Appl. Chem.* **1978**, *50*, 691.
(30) Weinberg, E. L.; Hunter, B. K.; Bairel, M. C. *J. Organomet. Chem.* **1982**, *240*, 95.

Chart I

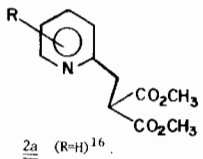

2a (R=H)[16]
2b (R=4-Me)[16]
2c (R=5-Me)[16]

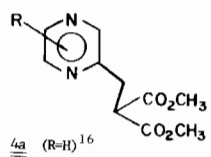

4a (R=H)[16]
4b (R=3-Me)[16]
4c (R=5-Me)[16]

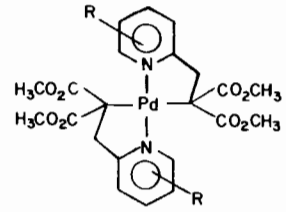

1a (R=H)[16]
1b (R=4-Me)[16]
1c (R=5-Me)[16]

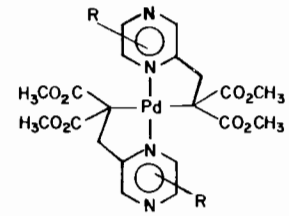

3a (R=H)[16]
3b (R=3-Me)[16]
3c (R=5-Me)[16]

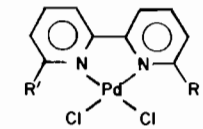

9a (R=R'=H)[68,69]
9b (R=H; R'=Me)[31]
9c (R=R'=Me)[31,67]
9d [R=R'=CH2CH(CO2Et)2]

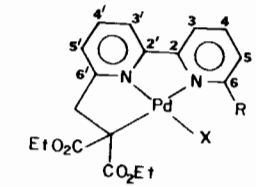

11a (R=H; X=Cl)
11b (R=Me; X=Cl)
11c [R=CH2CH(CO2Et)2; X=Cl]
11d [R=CH2CH(CO2Et)2; X=OAc]

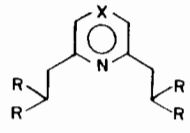

6a (R=CO2Me; X=CH)[65]
6b (R=CO2Me; X=N)[64]

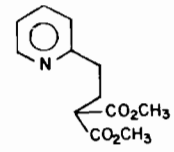

8[63]

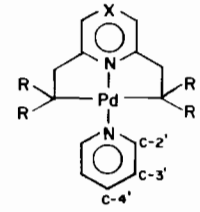

5a (R=CO2Me; X=CH)[65]
5b (R=CO2Me; X=N)[64]

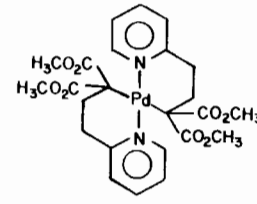

7[63]

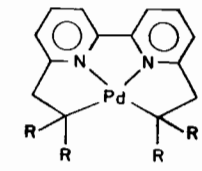

13a (R=CO2Me)
13b (R=CO2Et)[50]
13c (R=CO2ipr)

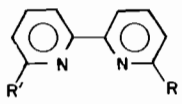

10a (R=R'=H)
10b (R=H; R'=Me)[59]
10c (R=R'=Me)[22,67]
10d [R'=CH2CH(CO2Et)2; R=H][62]
10e [R'=CH2CH(CO2Et)2; R=Me][62]
10f [R'=R=CH2CH(CO2Et)2]

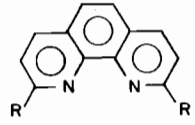

15a (R=H)
15b (R=Me)
15c [R=CH2CH(CO2Me)2]
15d [R=CH2CH(CO2Et)2]
15e [R=CH2CH(CO2ipr)2]

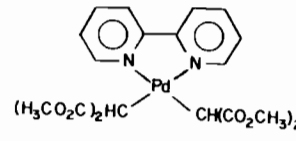

12[66]

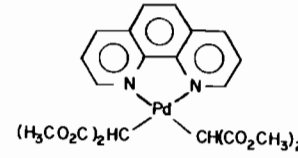

14[66]

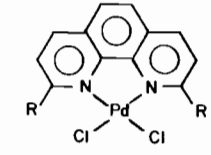

16a (R=H)[68]
16b (R=Me)
16c [R=CH2CH(CO2Me)2][70]

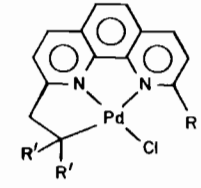

17a [R=CH2CH(CO2Me)2; R'=CO2Me]
17b [R=CH2CH(CO2Et)2; R'=CO2Et]
17c [R=CH2CH(CO2ipr)2; R'=CO2ipr]

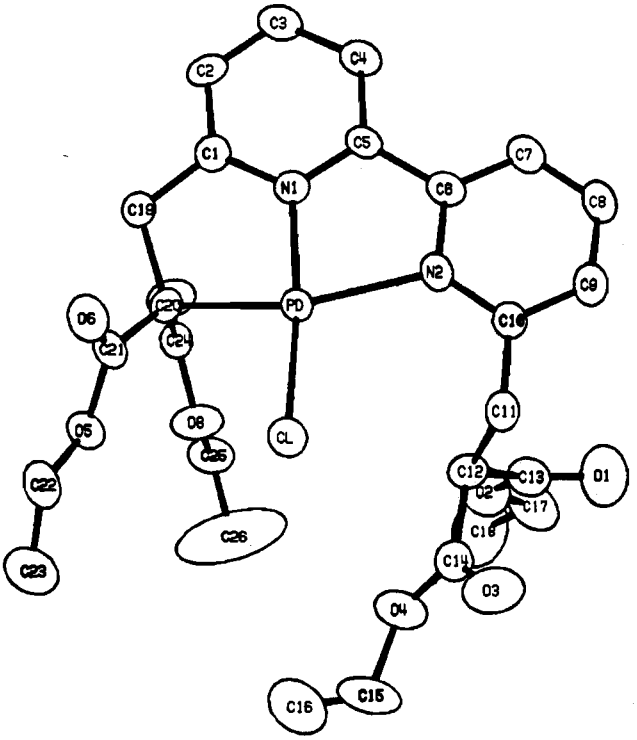

Figure 2. ORTEP drawing of **11c**.

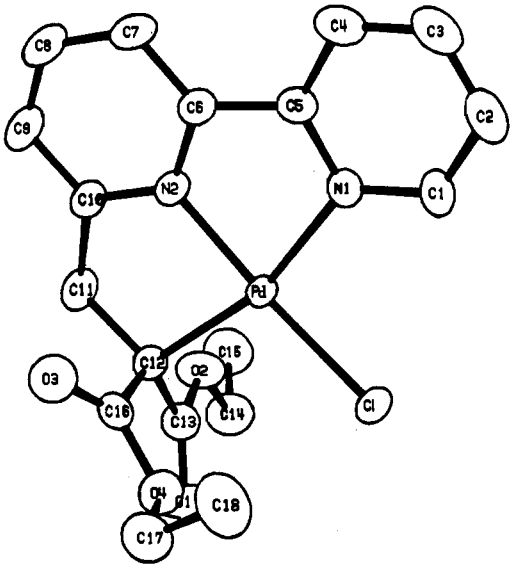

Figure 3. ORTEP drawing of **11a**.

importance of which should not be overestimated, since the ethyl analogue of **5a** also exhibited diastereotopic, nonequivalent methylene hydrogens. The ^{1}H NMR spectrum of **13b** does not change appreciably over a wide temperature range (25–100 °C). The degree of dissymmetry is diminished in the monometalated intermediates **11**, which exhibit a signal consisting of three quartets: one for the unbound side and two for the bound side. Similar spectral behavior is observed for **17b** and the unsymmetrical bipyridine analogues.

III. X-ray Structural Analysis. Several X-ray crystal structures have been determined for the key representative complexes and will be correlated with their corresponding ^{13}C NMR data in part IV. Of these X-ray structures, five are reported herein for the first time and discussed briefly in terms of the pivotal structural characteristics.

The crystal structure of initial adduct **9d**, derived from **10f** and palladium chloride, has been communicated,[31] with respect to the unexpected distortion taking place in the coordination sphere. The structure data of **9d** will be used as a comparative reference. In particular, the Pd–N bond distances (Table I) are of interest since they serve as the benchmark during the probe of the Pd–C bond character. Data comparisons of **9d** with **9a–c** is also instructive since **9c** and, to a lesser extent, **9b** possess an out-of-plane coordination and, further, the effect of the "ortho" substituent(s) generally results in a longer Pd–N bond length (than that of **9a**).

The structure of **11c** is depicted in Figure 2. There is considerable difference in the Pd–N bond lengths relative to **9d**. The shortened Pd–N1 bond can be attributed to the fact that this is the central bond in a 5.5-bicyclic ring system. The longer Pd–N2 distance is a direct effect of the strong trans influence of the coordinated C(sp^3) carbon and the steric repulsion of the chloride ligand with the adjacent alkyl group. In addition the Cl–Pd–N2 angle is significantly distorted from ideal (90°) at 106.2°, indicative of steric interactions with the juxtaposed uncoordinated carbon moiety. This latter aspect is well demonstrated in **11a** (Figure 3), which has no neighboring appendage and possesses a more idealized Cl–Pd–N1 angle of 97.24°.

The acetate intermediate **11d** (Figure 4) bears a close similarity to **11c** in most respects, including the dissymmetric orientation

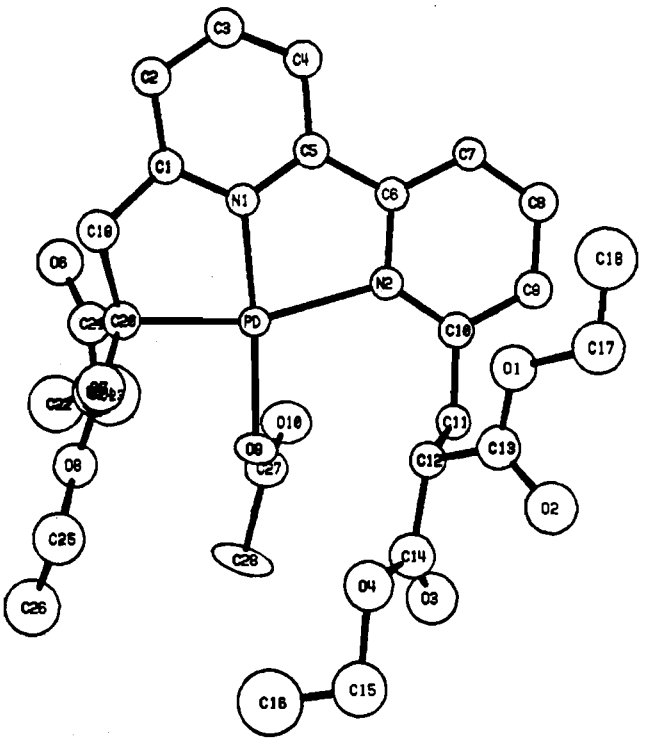

Figure 4. ORTEP drawing of **11d**.

of the pyridine rings around the metal.

In the crystal structure of **13b** (Figure 5), the ligand framework is nearly symmetrically disposed around the metal. In contrast to **11c**, both Pd–N1 and Pd–N2 lengths are equal, while the Pd–C bonds are slightly (~0.06 Å) longer than anticipated. The introduction of the second Pd–C bond in **13b** is accompanied by additional molecular distortions, which are most evident in the C(4)–C(5)–C(6) and C(5)–C(6)–C(7) angles being 125.9 and 126.7°, respectively. These expanded angles, relative to the other complexes, occur across the bipyridine linkage in order to accommodate the tetradentate coordination.

In the phenanthroline series, the solubility properties of the small alkyl esters dictated the use of higher branched alkyl groups; thus a successful single crystal of **17c** was grown. The most important feature derived from the X-ray data (Figure 6) is the decreased degrees of freedom around the metal resulting from the additional bridge. The distortions shown for **13b**, which lead to an overall tilt about the central 2,2′-bipyridine bond, are impossible for **17c**. The formation of the initial Pd–C bond distorts the remaining

(31) Newkome, G. R.; Fronczek, F. R.; Gupta, V. K.; Puckett, W. E.; Pantaleo, D. C.; Kiefer, G. E. *J. Am. Chem. Soc.* **1982**, *104*, 1782.

Table I. Important Bond Angles (deg), Bond Distances (Å), and ^{13}C NMR Chemical Shifts ($\Delta\delta$) in the Various Pd(II) Complexes

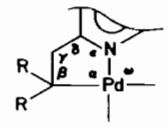

compds	bond angles					bond distance				^{13}C NMR			
	α (α′)	β (β′)	γ (γ′)	δ (δ′)	ϵ (ϵ′)	Pd–C (Pd–C′)	Pd–N1	Pd–N2	Pd–Cl (Pd–Cl′)	C2 (C2′)	C6 (C6′)	CH_2 ($C'H_2$)	C/CH (C′)
						Cis, No Pd–C Bond							
9a (R = R′ = H)	95.11 (94.01)						2.038	2.016	2.295 (2.271)	+1.5	+2.8		
9b (R = H, R′ = Me)	98.17 (93.70)						2.063	2.023	2.299 (2.299)	+0.5 (+2.3)	+3.1 (+9.6)		
9c (R = R′ = Me)	95.92 (96.15)						2.062	2.050	2.287 (2.292)	+1.4	+8.2		
9d (R = R′ = $CH_2CH(CO_2Et)_2$)	96.15 (94.62)						2.048	2.040	2.283 (2.286)	+0.5	+9.8	+1.1	0
16b (R = Me)	94.98 (95.03)						2.061	2.067	2.283				
16c (R = $CH_2CH(CO_2Me)_2$)	94.04 (96.36)						2.054	2.064	2.294 (2.283)	+2.4	+8.1	−0.3	+0.8
						Cis, One Pd–C Bond							
11a (X = Cl, R = H, R′ = CO_2Et)	83.5	105.9	113.0	113.4	119.4	2.083	1.949	2.088	2.290	+0.1 (−3.6)	+1.4 (+14.5)	+11.6	−4.2
11b (X = Cl, R = CH_3, R′ = CO_2Et)										−0.3 (−3.4)	+6.9 (+14.2)	+11.9	−3.5
11c (X = Cl, R = $CH_2CH(CO_2Et)_2$, R′ = CO_2Et)	82.6	106.1	112.1	114.1	118	2.089	1.971	2.205	2.313	−1.0 (−3.7)	+7.8 (+14.2)	+0.7 (+11.8)	+2.5 (−5.0)
11d (X = OAc, R = $CH_2CH(CO_2Et)_2$, R′ = CO_2Et)	83.8 (104.7)	107	111	116	118	2.066	1.969	2.184	2.047				
17c (X = Cl, R = $CH_2CH(CO_2$-*i*-Pr$)_2$, R′ = CO_2-*i*-Pr)	82.1	105.6	111.9	112.6	120.3	2.089	1.956	2.225	2.286	+1.0 (−2.1)	+6.2 (+10.6)	−0.7 (+11.3)	+2.0 (−5.6)
						Cis, Two Pd–C Bonds							
12 (R = $CH(CO_2Me)_2$)										−0.4	+4.3		+12.5
13b (R = CO_2Et)	81.5 (82.5)	105.3 (103.6)	112.4 (112.0)	113.2 (113.8)	119.9 (119.8)	2.141 (2.152)	1.983	1.979		−4.1	+14.6	+12.2	−3.0
14										+0.3	+3.4		+12.9
						Trans, Two Pd–C Bonds							
1a (R = H)	79.6 (80.3)	100.3	110.7 (110.1)	114.2 (114.9)	125.6	2.156 (2.142)	2.040	2.042		+14.8	+3.1	+7.4	+3.7
1b (R = 4-Me)										+13.7	+1.8	+6.5	+2.4
1c (R = 5-Me)										+13.5	+1.7	+6.1	+2.0
3a (R = H)										+13.4	+0.1	+7.3	+4.9
3b (R = 3-Me)										+12.7	+2.0	+7.7	+4.0
3c (R = 5-Me)										+11.4	+0.7	+7.1	+4.2
7	83.9 (84.5)	107.4 (109.9)	111.0 (114.4)	116.0 (116.3)	120.3 (119.7)	2.190 (2.172)	2.038	2.037		+2.5	+1.9	+7.1 (+0.4)	−5.2
5a (X = CH)	81.8	102.8	111.1	114.5	120.2	2.140	1.967	2.050		+13.6 (+1.2)		+7.2	+1.3
5b (X = H)										+13.7 (+1.3)		+ 7.9	+2.2

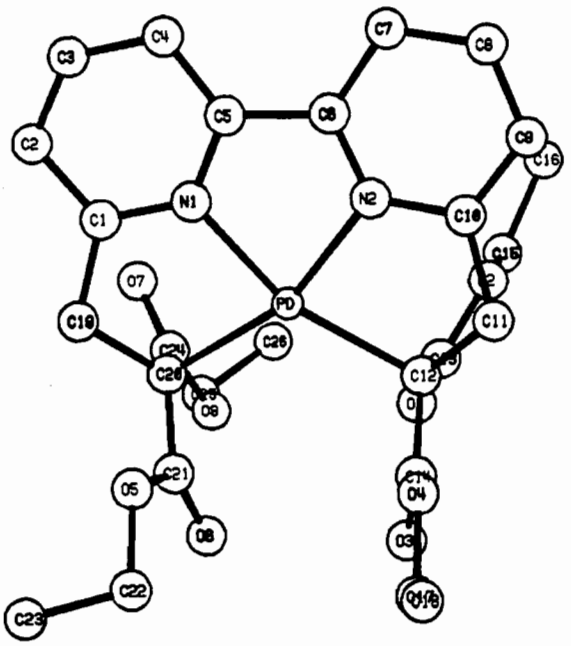

Figure 5. ORTEP drawing of **13b**.

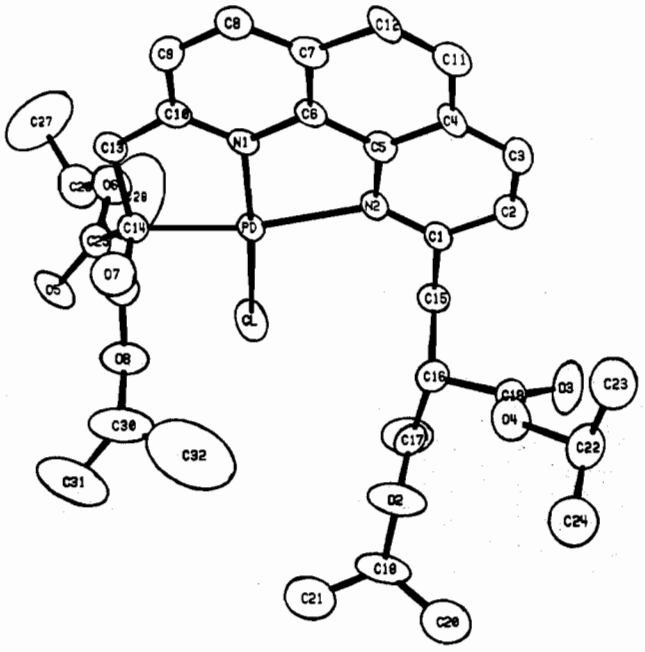

Figure 6. ORTEP drawing of **17c**.

structure sufficiently to prevent approach of the second carbanion.

IV. ^{13}C NMR Spectral Results. In all complexes herein described, the sp^3 carbons are easily assigned from multiplicity information gained via either off-resonance double-resonance proton-coupled spectra or preferably the NOE enhanced nondecoupled ^{13}C spectra. Multiplicity change (2:1 line pattern) for the coordinating carbon is helpful in its assignment even though the signal intensity is sacrificed by the loss of NOE. Ambiguities from the carbon resonance multiplicities are for (1) the ethyl esters, where the α-heteroaryl and ester methylenes both show three-line patterns, (2) bridging methylenes in **7**, and (3) the unsubstituted heteroaromatic carbons. The problem is easily resolved on the basis of chemical shift, e.g., pyrCH_2 (~32–43 ppm) vs CH_2CH_3 (~50–52 ppm). The bridging methylenes of **7** are distinguished upon complexation by the Δ values 17.1 and 0.4 ppm for pyCH_2CH_2 and pyCH_2CH_2, respectively. The C=O carbons always occur the farthest downfield and are typified by the low signal intensity.

The ^{13}C NMR spectrum of **7** gives two signals for both the C=O and OCH_3 groups. This dissymmetry, exhibited by the ester moieties, arises because of a conformationally rigid "equatorial–axial" orientation of the methoxycarbonyl groups on the six-membered metallacyclic ring.

Assignments of the heteroaryl carbons in **1**, **3**, **5**, and **7** can be made by comparison with literature values for related analogues.[22,32–34] Some difficulties were encountered in the C3 and C5 assignments for **1a–c**; however, confirmation is deduced via the methyl substitution at C5 in **1c** providing a steric shift for that carbon signal. Selective single-frequency decoupling with NOE was required to designate the closely spaced heteroaromatic signals in **3**, whereas the signals from **9** and **12** were assigned by first-order spectral comparisons. Fortuitously, the spectral pattern for **9b** was a unique composite of data for **9a** and **9c**. The ^{13}C NMR spectral data for the **11** species were difficult to assign because of their innate dissymmetry. However, **9d**, **11c**, and **13b** were compared and assigned in a manner analogous to that for **9b**. For aromatic carbons, complex **11c** exhibited a 10-line pattern that was an exact superposition of the two 5-line patterns for **9d** and **13**. Spectra for **11a** and **11b** were assigned by analogy.

The phenanthroline complexes **16a** and **16b** posed a special problem due to their insolubility in most NMR solvents. Assignments[35] were completed as described above on only the more soluble complexes **14**, **16c**, and **17a**. INEPT and selective single-frequency decoupling with NOE further insured the proper identification.

V. Infrared Spectral Features. The vibrational bands resulting from the heteroaromatic ligands and their Pd(II) complexes are delineated in the supplementary material. From these complexes, only a representative example of each complex is presented because of spectral similarities. The assignments of the various IR bands resulting from the heteroaromatic part in the ligands/complexes have been done on the basis described by Katritkzy[36] and others.[37–41]. The salient features from the IR data are *position, intensity, and splitting of bands.*

There is a considerable shift and intensification of the various vibrational bands of different electron-deficient heteroaromatics as a result of complexation. Band splitting is observed especially in the monometalated and cis complexes.

The free ligands (e.g., **2a**, **4a**, **6a**, **8**, **10e**, **10f**, and **15c**) show C=O stretching bands at 1730–1750 cm^{-1} and at 1640–1680 cm^{-1} for the corresponding complexes indicative of Pd–C bond formation. This is in accordance with the Pd(II) complex of acetylacetone, which shows ν(C=O) at 1665 (vs) and 1632 (vs) cm^{-1} due to the Pd–C bond and at 1572 (vs) and 1523 (vs) cm^{-1} due to the chelated enolate group.[42] In **9d** and **16c**, this frequency is unaffected as expected, while the monometalated complexes **11c** and **17a** show a mixed pattern.

The absorption in the 1600–1300-cm^{-1} region is principally due to ring stretching vibrations, and all complexes exhibit a series of strong bands in this region. The shoulders and splitting of bands in this region are distinct features of cis complexes having one or no C–Pd bonds.

In the cis complexes, two weak-intensity bands at 1280–1300 and 1260–1275 cm^{-1} are assigned to the ring stretching vibrations while a band appearing at ca. 1240 cm^{-1} is assigned to the re-

(32) Johnson, L. F.; Jankowski, W. C. "Carbon-13 NMR Spectra"; Wiley-Interscience: New York, 1972.
(33) Breitmaier, H.; Voelter, G. "Atlas of Carbon-13 NMR Data"; Heyden: Philadelphia, 1979.
(34) "Sadtler Standard Carbon-13 NMR Spectra"; Sadtler Research Laboratories: Philadelphia, 1980.
(35) Chandler, C. J.; Deady, L. W.; Reiss, J. A. *J. Heterocycl. Chem.* **1981**, *18*, 599.
(36) Katritzky, A. R.; Ed. "Physical Methods in Heterocyclic Chemistry"; Academic Press: New York, 1963; Vol. II, Chapter 2.
(37) Lord, R. C.; Marston, A. L.; Miller, F. A. *Spectrochim. Acta* **1957**, *9*, 113.
(38) Strukl, J. S.; Walter, J. L. *Spectrochim. Acta, Part A* **1971**, *27A*, 223.
(39) Grigg, E. C. M.; Hall, J. R.; Plowman, R. A. *Aust. J. Chem.* **1962**, *15*, 425.
(40) Inskeep, R. G. *J. Inorg. Nucl. Chem.* **1962**, *24*, 763.
(41) Schilt, A. A.; Taylor, R. C. *J. Inorg. Nucl. Chem.* **1959**, *9*, 211.
(42) Baba, S.; Ogura, T.; Kawaguchi, S. *Inorg. Nucl. Chem. Lett.* **1971**, *7*, 1195.

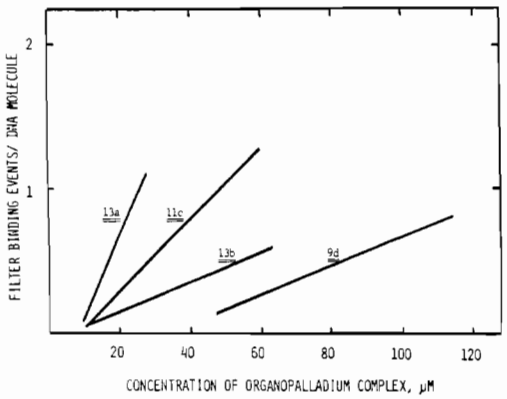

Figure 7. Structure–activity profile. Reaction mixtures are described in the Experimental Section. Experimental points represent the amount of phage PM2 DNA trapped on nitrocellulose filters due to the binding of DNA of the individually tested complexes. The best-fit line was calculated from linear-regression analysis using six different concentrations for each complex.

sonant-dependent ring stretching mode. The remaining bands in this region in all complexes are attributed to the hydrogen in-plane bending mode.

The 1100–600-cm^{-1} region exhibits the remaining in-plane hydrogen bending motions and ring stretching plus bending vibrations. The characteristic aromatic out-of-plane substitution-dependent hydrogen modes are also shown by their strong absorptions. It is interesting that the ring breathing motion is shifted about 30 cm^{-1} to higher frequencies in the Pd(II) complexes; similar trends have been observed for other metal chelates.[38,40,41,43]

For a large number of related *N*-imine complexes of Pd(II), Durig et al.[44,45] and others[46] reported that the Pd–N stretching frequency appears in the 450–500-cm^{-1} region. Thus the bands in the 445–504-cm^{-1} region (these are absent in the ligand spectra) were assigned to the Pd–N stretching vibrations. Complexes **14**, **16**, and **17** show these motions at a slightly higher wavenumber than the other complexes. The cis complexes showed two bands for ν(Pd–N) while the trans complexes exhibited but one.

Lack of literature data on the Pd(II)–C(sp^3) stretching frequency imposes a major limitation. Kawaguchi et al.[42] reported the Pd–C stretching mode in the Pd(II) complex of acetylacetone at 540 cm^{-1}; however, in the complexes reported herein new bands appear in the 370–415-cm^{-1} region and are tentatively assigned to ν(Pd–C) motion. Two bands were also observed in cis complexes and one in trans complexes.

The Pd–Cl stretching frequencies[44-46] were found in the region from 320 to 354 cm^{-1}, which is a much smaller range than that found for the Pd–N stretching vibrations. The cis complexes with one or two Pd–Cl bonds also exhibit two bands in this region.

VI. Biochemical Aspects. Interaction of Pd–C Complexes with Phage PM2 DNA⁺. A. Filter-Binding Assays. The results of these assays with **9d**, **11c**, **13a**, and **13b** are shown in Figure 7. There is a clear difference in the level of DNA binding with each individual complex over the concentration range tested. The adduct **9d** (no Pd–C bond) exhibits low levels of DNA association at complex concentrations less than 40 μM. When Pd–C bonds are introduced, an increased level of DNA–complex association is generally observed. For example, the binding of **13b** to DNA can be detected at significantly lower concentrations than that of **9d**.

B. Inhibition of Filter-Binding Events. Filter-binding events (nicking) of PM2 DNA incubated with **13b** were either inhibited or reversed in the following cases: (1) Addition of 2-mercaptoethanol (10 mM), dithiothreitol (10 mM), or thiourea (10 mM) to the cocktail resulted in the complete inhibition of **13b** binding to DNA in which concentrations of **13b** ranged from 20 to 60 μm. (2) Addition of NaCl (500 mM) inhibited the filter-binding events. (3) Prolonged exposure (17 h) to alkali following incubation *reversed* the filter-binding events.

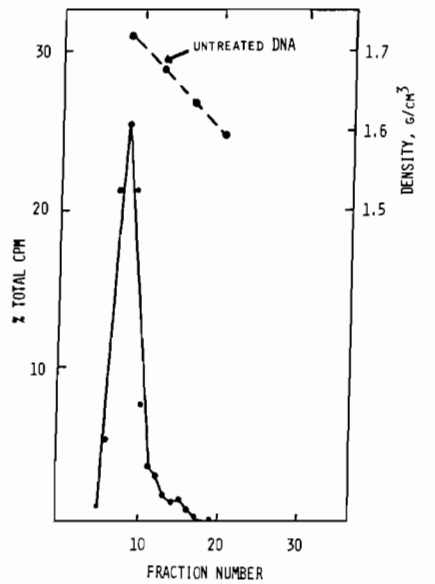

Figure 8. Gradients in CsCl of phage PM2 [^{3}H]DNA treated with **13b** (40 μm). The arrow indicates untreated, form I, PM2 [^{3}H]DNA.

Table II. Nick Translation on PM2 DNA Treated with 13b[a]

concn of 13b, μM	[^{3}H]dATP incorporated per DNA molecule, fmol
0.1	10
0.2	23
0.5	9
1.0	6
4.0	4
10.0	2
20.0	<1

[a] Reaction mixtures were as described in the Experimental Section in which 80 fmol of PM2 DNA molecules were reacted with **13b** at the above concnetrations. Approximately 5 fmol of [^{3}H]dATP was incorporated per DNA molecule in the absence of **13b** and is considered to be part of the overall incorporation depicted above.

C. Buoyant Density Determination. A significant shift in density was observed when PM2 DNA was incubated with **13b** (40 μM). The refractive index of the fraction representing maximal recovery of radioactivity (Figure 8) was used to calculate band density.[47] The calculated density of unreacted PM2 DNA (1.685 g/mL) was close to the value of 1.694 g/mL reported[48] as the density of PM2 DNA I. The band representing PM2 DNA reacted with **13b** in a buoyant density of 1.720 g/mL or an increment of 35 mg/mL. Form II DNA is reported to have a buoyant density 14.8 mg/mL less than that of form I. The gradient profiles failed to show any detectable conversion to form II DNA.

D. Priming Activity of PM2 DNA. In order to determine the biological consequences of **13b** acting on PM2 DNA, the ability of *Escherichia coli* DNA polymerase I to catalyze DNA synthesis on a template reacted with **13b** was evaluated. An absolute criterion for detecting DNA synthesis would be that **13b** either produce an appropriately nicked-primer template or stimulate DNA polymerase I activity at naturally occurring nicks.[49] As

(43) Sinha, S. P. *Spectrochim. Acta* **1964**, *20*, 879.
(44) Durig, J. R.; Layton, R.; Sink, D. W.; Mitchell, B. R. *Spectrochim. Acta* **1965**, *21*, 1367.
(45) Perry, C. H.; Athens, D. P.; Young, E. F.; Durig, J. R.; Mitchell, B. R. *Spectrochim. Acta, Part A* **1967**, *23A*, 1137.
(46) Hendra, P. J. *Spectrochim. Acta, Part A* **1967**, *23A*, 1275.
(47) Vinograd, J.; Hearst, J. E. *Prog. Org. Chem. Nat. Prod.* **1962**, *20*, 372.
(48) Bauer, W.; Gonias, S. L.; Kam, S. K.; Wu, K. C.; Lippard, S. J. *Biochemistry* **1978**, *17*, 1060.
(49) Kelly, R. B.; Cozzarelli, N. R.; Deutscher, M. P.; Lehman, I. R.; Kornberg, A. *J. Biol. Chem.* **1970**, *245*, 39.

Table III. ^{13}C NMR Spectral Data of Square-Planar Trans-Palladated Complexes of Pyridine- and Pyrazine-Based Ligands[a]

compd	C-2(2′)	C-3(3′)	C-4(4′)	C-5	C-6	C=O	CH_2	OCH_3	C/CH	ring CH_3	ref
1a	171.8	120.6	138.0	121.2	151.7	173.7	43.1	51.0	53.6		16
2a	[157.0]	[122.7]	[135.7]	[121.0]	[148.6]	[168.8]	[35.7]	[51.7]	[49.9]		
1a	171.0	121.2	149.8	122.2	150.8	173.8	42.8	50.8	53.1	21.1	16
2b	[157.3]	[124.3]	[147.4]	[122.6]	[149.0]	[169.6]	[36.3]	[52.5]	[50.7]	[20.8]	
1c	168.0	119.7	138.3	130.4	151.2	173.4	42.1	50.3	52.9	17.5	16
2c	[154.5]	[122.8]	[136.8]	[130.0]	[149.5]	[169.5]	[36.0]	[52.4]	[50.9]	[17.9]	
3a	166.5	143.1		143.2	144.4	172.6	40.5	51.2	54.6		16
4a	[153.1]	[144.7]		[142.3]	[143.4]	[168.7]	[33.2]	[52.2]	[49.7]		
3b	165.0	154.5		142.2	142.6	173.1	40.2	51.3	52.6	23.3	16
4b	[152.3]	[151.3]		[141.2]	[140.6]	[169.3]	[32.5]	[52.2]	[48.6]	[21.1]	
3c	162.8	141.9		152.6	144.0	173.0	40.0	51.1	54.3	21.3	16
4c	[151.4]	[143.3]		[149.8]	[143.3]	[168.9]	[32.9]	[52.3]	[50.1]	[20.7]	
5a	169.6	117.8	138.0			172.1	42.8	50.6	51.0		65
	(151.0)	(123.6)	(137.0)								
6a	[156.3]	[120.7]	[136.2]			[169.1]	[35.6]	[51.8]	[49.7]		
	(149.8)	(123.6)	(135.7)								
5b	165.8	140.3	(137.6)			172.0	40.8	50.9	51.6		64
	(151.1)	(124.1)									
6b	[152.1]	[142.3]				[168.9]	[32.9]	[52.2]	[49.4]		
	(149.8)	(123.6)	[(135.7)]								
7	162.8	122.3	137.6	121.5	151.3	175.9/173.7	42.4/28.6	50.5/49.6	45.6		63
8	[160.3]	[122.9]	[136.4]	[121.3]	[149.4]	[169.7]	[35.3/28.2]	[52.2]	[50.8]		

[a] Brackets designate signals for the corresponding ligands.

seen in Table II, DNA synthesis is observed, in which maximal activity is detected on a DNA substrate treated with **13b** (0.2 μM). Template-primer activity drops sharply at concentrations of **13b** either above or below 0.2 μM. In fact, at concentrations greater than 1 μM, DNA synthesis drops to levels below that observed for nontreated DNA.[50]

The inability to detect form II DNA in CsCl gradients suggests that the transient increase of DNA synthesis observed is more than likely due to a stimulation of DNA polymerase I activity and not to **13b** introducing additional primer termini into DNA. On the other hand, our results are consistent with **13b** binding to DNA, eventually creating a roadblock for the DNA polymerase and thus causing inhibition of nick translation.

Previous reports indicated that **13b** produced phosphodiester breaks in DNA.[51] This has not been substantiated by experiments reported here or by other techniques such as agarose gel electrophoresis. It is conceivable that binding of **13b** to DNA could have compromised assays to detect nicks in DNA, although the levels of binding to DNA at a specific concentration of **13b** are always less than the results obtained by measuring phosphodiester breaks. The rationale for these inconsistencies is unclear but implies that an artifact peculiar to these complexes is being introduced into the assay for measuring nicks in PM2 DNA.

Discussion

^{13}C NMR Spectral Correlations. The trans complexes (**1**, **3**, **5**, **7**) can be divided into two general categories: (1) those possessing two isolated rings (**1**, **3**, **7**) and (2) those having two cumulated metallacyclic rings (**5**). Inspection of Table III reveals almost identical ^{13}C chemical shift differences for either cyclometalated ring species. Upon Pd–C bond formation, the α-heteroaryl methylene is shifted downfield by $\Delta\delta$ = 6.0–7.9 for all trans complexes. The coordinated carbon in **1**, **3**, and **5** shifts downfield to a lesser extent ($\Delta\delta$ = 1.3–4.9), whereas **7** exhibits the exception by an upfield shift ($\Delta\delta$ = 5.2). The rationale for this anomalous behavior will be considered later. The metallacyclic ring carbon C2 shows the largest shift, $\Delta\delta \approx 13$; complex **7** is again the exception. Interestingly, in the unchelated pyridine ring of **5**, the small $\Delta\delta \approx 1.2$ is realized for C2′, indicating that cyclometalation plays an important role in the large C2 chemical shift. As for the other heteroaromatic carbons in **1**, **3**, and **5**, the chemical shifts of C3 are upfield ($\Delta\delta \approx 1.4$–3.1), except for **3b**. C4 and C6 are downfield, and C5 is essentially unchanged. Complex **7** is again the exception to the trends.

The adducts, which do not possess a Pd–C bond, show similar $\Delta\delta(^{13}C)$ shift values for the heteroaromatic carbons. Alkyl-substituted positions, such as 6′ in **9b–d** and **16c**, are shifted markedly downfield by 8–10 ppm.[52] In all cis complexes, C3 and C5 are shifted downfield with C5′ noticeably (≥4 ppm) affected in **9b–d** and in **16c**. Similarly, C4 experienced a downfield shift by $\Delta\delta$ 2–4 as does C2 ($\Delta\delta \leq 2.4$). Alkyl substituents on these adducts show small to negligible shifts. In complexes **12** and **14**, the metalated carbons show a large downfield shift of $\Delta\delta$ = 12.5–12.9 mainly due to the change from CH_2 to CH.

Complexes **11**, **13**, and **17** contain at least one cyclometalated ring. For these complexes the α-heteroaryl methylene carbon in the chelate ring has a large downfield shift ($\Delta\delta$ ca. 12 ppm) as in the trans analogues but about double in magnitude, whereas the coordinated carbon is shifted *upfield* ($\Delta\delta$ = 3–5.6). The heteroaromatic C6′, analogous to C2 in the trans series, has a $\Delta\delta$ = 14 downfield shift, while C2′ is slightly upfield ($\Delta\delta$ = ca. 3.4) and C2 for **11a–c** and **17** are constant. For the nonmetalated side in **11a–c**, signals for C3 and C5 are shifted downfield by average values of $\Delta\delta$ = 1.7 and 4.9, respectively, while there is no significant change in C3′ and C5′ (chelated side) in **11a–c** or none in C3–C5 in **13**. C4 is shifted downfield ($\Delta\delta$ = 2–4) in all cis complexes (Table IV and V).

The various $\Delta\delta(^{13}C)$ NMR values for these complexes have been rationalized via two general terms that account for the chemical shifts encountered upon coordination and subsequent cyclometalation. The "strain effects" will be used to describe bond angle perturbations, whereas "electronic effects" will describe the purely electron density changes that influence chemical shift.

The coordinated carbon in these complexes gives different $\Delta\delta(^{13}C)$ values for the trans vs. the cis series despite the fact that

(50) A certain proportion of the unlabeled DNA substrate contains nicks. By the use of 1% agarose gels we estimate that approximately 10% of the DNA substrate contained nicks (90% form I, 10% form II), some or all of which could presumably be used as a primer template for DNA polymerase I synthesis. Our results indicate that nick translation even at these naturally occurring sites is inhibited by high concentrations of **13b**.

(51) Newkome, G. R.; Onishi, M.; Puckett, W. E.; Deutsch, W. A. *J. Am. Chem. Soc.* **1980**, *102*, 4551.

(52) Standard numbering for phenanthroline does not correlate with that for bipyridine; however, the related positions appear in the appropriate column (Tables IV and V).

Table IV. ^{13}C NMR Spectral Data of Square-Planar Cis-Palladated Complexes of 2,2'-Bipyridine-Based Ligands[a]

compd	C-2(2')	C-3(3')	C-4(4')	C-5(5')	C-6(6')	C=O (C'=O)	CH_2 ($C'H_2$)	OCH_2 ($OC'H_2$)	CH_3 ($C'H_3$)	C/CH (C')	(ring $C'H_3$)	ref
9a	157.3	122.5	139.3	125.8	151.6							68, 69
12	155.4	121.6	138.9	126.4	153.1	174.8			50.9	52.4		66
10a	[155.8]	[120.7]	[136.4]	[123.3]	[148.8]	[166.2][b]			[51.2][b]	[39.9][b,c]		
9b	156.5	122.5	139.3	125.8	151.6							31
	(157.3)	(119.8)	(140.0)	(128.9)	(166.8)						(28.3)	
10b	[156.0]	[120.5]	[136.1]	[122.9]	[148.5]							
	[(155.0)]	[(117.5)]	[(136.4)]	[(122.6)]	[(157.2)]						[(24.1)]	22, 59
9c	157.2	119.6	139.6	127.0	165.8						27.2	31, 67
10c	[155.8]	[117.9]	[136.7]	[122.8]	[157.6]						[24.4]	22
9d	157.1	121.7	140.9	127.2	164.8	168.0	36.9	61.6	13.8	52.0		
11c	155.6	120.8	139.5	128.9	162.8	168.3	36.5	61.1	13.8	52.9		
	(152.9)	(119.2)	(139.0)	(122.3)	(169.2)	(173.6)	(47.6)	(60.4)	(14.2)	(45.4)		
13b	152.5	118.6	138.6	122.5	169.6	173.8	48.0	59.3	14.3	47.4		
10f	[156.6]	[118.5]	[136.8]	[122.9]	[155.0]	[169.1]	[35.8]	[61.0]	[13.8]	[50.4]		
11a	155.2	121.9	139.6	126.7	150.3	174.1	47.5	60.7	14.5	46.4		
	(152.5)	(118.5)	(138.6)	(123.1)	(171.4)							
10d	[155.1]	[121.1]	[136.6]	[123.5]	[148.9]	[169.3]	[35.9]	[61.2]	[13.9]	[50.6]		62
	(156.1)	(118.5)	(137.1)	(123.2)	(156.9)							
11b	154.8	119.4	139.0	128.0	164.1	173.5	47.5	60.4	14.2	46.7	26.7	
	(153.0)	(118.6)	(138.6)	(122.0)	(169.3)							
10e	[155.1]	[117.6]	[136.3]	[122.6]	[157.2]	[168.9]	[35.6]	[60.8]	[13.6]	[50.2]		62
	(156.4)	(118.2)	(136.5)	(122.6)	(155.1)						(24.0)	

[a] Brackets designate signals for the corresponding ligands. [b] Free dimethyl malonate. [c] CH_2.

Table V. ^{13}C NMR Spectral Data of Square-Planar Cis-Palladated Complexes of Phenanthroline-Based Ligands[a]

compd	C-10a-(10b)	C-4a(4b)	C-4(7)	C-3(8)	C-2(9)	C=O	CH_2	C-5(6)	CH_3	C/CH	ref
14	146.0	129.3	137.8	125.2	153.2	174.9		126.9	50.9	52.8	66
15a	[145.7]	[128.2]	[135.5]	[122.5]	[149.8]	[166.2][b]		[126.0]	[51.2][b]	[39.9][b,c]	
16c	147.9	128.6	139.6	127.3	166.2	168.6	36.9	126.7	52.6	51.5	70
17a	146.5	128.4	138.2	128.2	164.3	169.8	36.5	126.6	52.3	52.7	
	(143.4)	(127.2)	(137.1)	(122.0)	(168.7)	(174.4)	(48.5)	(125.8)	(51.9)	(45.1)	
15c	[145.5]	[127.4]	[136.3]	[123.3]	[158.1]	[170.0]	[37.2]	[125.8]	[52.4]	[50.7]	

[a] Brackets designate signals for the corresponding ligands. [b] Free dimethyl malonate. [c] CH_2.

all complexes (except **7**) possess five-membered rings, have identical substitution at the coordinated carbon, and are bound to Pd(II). Inspection of the X-ray data reveals subtle structural differences between these series such as the N–Pd–C (α) angle. The average trans and cis C–C–Pd (β) angles are 100.3 and 104.5–106.1°, respectively. Interestingly, the ^{13}C chemical shift of the identically substituted coordinated carbons varies drastically between the cyclic and acyclic complexes.[53,54] Thus, stereochemical and strain energy differences must have considerable impact on the chemical shift, which is also dependent on the metal–ligand substitution pattern. Generally, ^{13}C chemical shifts for sp^3 carbons coordinated to Pd(II) range from 90 to 100 ppm when the secondary ligand ranges in ligandophilicity from PAr_3 to pyridine.[55] By restriction of the complex's structural modifications to a narrow range, minimum gross electronic effects on the $\Delta\delta$ (^{13}C) values should be realized. Thus, electronic effects per se appear to play a negligible role since the $\Delta\delta(^{13}C)$ values are not dramatically affected either by change of the cis substituents (e.g., C in **13** or Cl in **9**) or by the "trans effect". Further, the coordinated carbon $\Delta\delta(^{13}C)$ values of 5.2 and 3.0 for **7** and **13b**, respectively, are similar; β for **7** is 108.6°, which is larger than that found in other trans complexes due to the six-membered chelate ring *and* similar to that found in the cis complexes. The α-heteroaryl methylene in the trans series has nearly an "ideal" γ angle of 110.6° while those of the cis series average 112°; thus the larger downfield shift for the cis series can be directly related to an increased bond angle. The electronic effects cannot be assessed because of the similarity in both series.

Large $\Delta\delta(^{13}C)$ values for the trans vs. cis heteroaromatic C2 and C6 positions were noted. In both series the δ angle averages 114°, whereas **7** shows a small $\Delta\delta(^{13}C)$ value (~2) for this mutual carbon and a δ angle of 116°, which is close to ideal (120°). Bond angle strain at C6 can be shown to affect the chemical shift in at least the noncyclometalated examples. Comparison of C6 in complexes **9** and **16c** shows that when changes in the bond angle or other geometric deviations take place, $\Delta\delta(^{13}C)$ generally increases. Complex **9a** has nearly ideal geometry (that is, square-planar metal and planar bipyridine) and has relatively small $\Delta\delta(^{13}C)$ values for all heteroaryl carbons. The subtle deviations can be assigned to purely electronic effects; however, when steric interactions cause severe geometric deviations as in **9c–e** and **16b–c**, large $\Delta\delta(^{13}C)$ values are noted—especially at C6.[31]

Discussion for Biological Assays

The biochemical assays indicate binding of the complexes to DNA occurs. The exact nature of this binding is unknown, although experiments described here suggest an intercalative mode of binding; e.g., the inhibition of filter-binding events by thiols could be due to a change in the geometry of **13b** from square planar to octahedral. If it is true that the square-planar structure is required, then this result, along with the inhibition by high salt concentration, is consistent with DNA intercalation. An increase in density of DNA would also occur by this mode of action, as has been observed for pSMI incubated in the presence of platinum uracil blue.[48]

Conclusions

Relating ^{13}C data to "steric" and "electronic" effects in bi- and tridentate alkylamine complexes is precedented.[56] Those authors[56]

(53) Wiger, G.; Albelo, G.; Rettig, M. F. *J. Chem. Soc., Dalton Trans.* **1974**, 2242.
(54) Goddard, R.; Green, M.; Hughes, R. P.; Woodward, P. *J. Chem. Soc., Dalton Trans.* **1976**, 1890.
(55) Mann, B. E. *Adv. Organomet. Chem.* **1974**, *12*, 135.

Table VI. Crystal Data for 11a, 11c, 11d, 13b, and 17c

	$PdClC_{18}H_{19}N_2O_4$	$PdClC_{26}H_{31}N_2O_8$	$PdC_{28}H_{34}N_2O_{10}$	$PdC_{26}H_{30}N_2O_8 \cdot KNO_3 \cdot {}^1/_2EtOAc$	$PdClC_{32}H_{39}N_2O_8$
fw	469.2	641.4	665.0	750.1	721.5
cryst syst	monoclinic	monoclinic	triclinic	monoclinic	triclinic
space group	$P2_1/n$	$P2_1/c$	$P\bar{1}$	$C2/c$	$P\bar{1}$
a, Å	7.573 (3)	18.909 (3)	11.996 (3)	20.161 (4)	9.425 (2)
b, Å	18.746 (5)	8.900 (1)	16.402 (6)	17.991 (4)	9.811 (2)
c, Å	12.962 (2)	16.684 (3)	17.214 (5)	17.995 (2)	20.510 (5)
α, deg			116.62 (3)		78.98 (2)
β, deg	90.86 (3)	94.86 (1)	95.05 (2)	109.16 (2)	78.48 (2)
γ, deg			94.54 (3)		66.57 (2)
V, Å^3	1840 (2)	2798 (1)	2989 (4)	6166 (4)	1692 (1)
Z, formula units/cell	4	4	4	8	2
D_{calcd}, g/cm^3	1.694	1.523	1.477	1.616	1.416
μ(Mo Kα), cm^{-1}	11.63	8.00	6.66	7.92	6.67
cryst size, mm	0.16 × 0.36 × 0.60	0.20 × 0.40 × 0.56	0.08 × 0.42 × 0.48	0.08 × 0.08 × 0.24	0.08 × 0.20 × 0.28
color	yellow	orange	yellow	yellow	yellow
temp, °C	24	25	23	23	26
θ limits, deg	$2 < \theta \leq 25$	$2 < \theta < 25$	$1 < \theta < 20$	$1 < \theta < 20$	$1 < \theta < 22.5$
scan speed, deg/min	0.33–5.0	0.33–10.0	0.60–20.0	0.31–4.0	0.65–5.0
precision	$I \cong 50\sigma(I)$	$I \cong 50\sigma(I)$	$I \cong 20\sigma(I)$	$I \cong 25\sigma(I)$	$I \cong 20\sigma(I)$
min. transmission coeff, %	66.42	94.81	88.73		84.62
unique data	3215	4910	5554	2869	4410
obsd data	2556	3573	2452	1897	3015
criterion for obsd data	$I > 3\sigma(I)$	$I > 3\sigma(I)$	$I > 3\sigma(I)$	$I > 2\sigma(I)$	$I > 3\sigma(I)$
refined variables	235	343	379	183	397
R	0.031	0.031	0.061	0.074	0.041
R_w	0.042	0.046	0.068	0.083	0.052
residual density, e/Å^3	0.64	0.75	0.35	0.85	0.55

presented evidence that carbons in a five-membered chelate ring resonate at *lower* field than those of a six-membered homologue because the bond angles and lengths in a five-membered chelate rings are very close to "ideal" values. The carbons within a six-membered chelate then resonate at *higher* field because of steric perturbations associated with nonideal bond angle distortions.

We, however, have presented evidence that (1) the bond angles and lengths for cyclometalated six-membered rings are much *closer* to ideal than those of the related five-membered chelates, yet some of the six-membered chelate carbons still resonate at higher field than their five-membered counterparts, (2) the stereochemistry of the chelate ring is the most important factor in determining chemical shift, as has been suggested in other systems, and (3) not all five- and six-membered chelates will show similar stereochemical distortions.

Pyridine ring ^{13}C chemical shifts have been shown to correlate with calculated (CNDO) electron densities and Hammett substituent constants.[19] The correlation of $\Delta\delta(^{13}C)$ and chemical shift with bond angle for several related pairs of data points is shown in Figure 9. A good linear fit was found for the chemical shift of the coordinated carbon vs. the Pd–*C*–CH_2 bond angle (complexes **7** and **17a** were omitted from the regression calculation). Carbon–Pd distance vs. chemical shift data failed to give a reasonable correlation.

We have been able to correlate ^{13}C chemical shift data with structural parameters of closely related Pd(II) complexes. Our work is continuing into structural and spectral relationships in modified complexes.

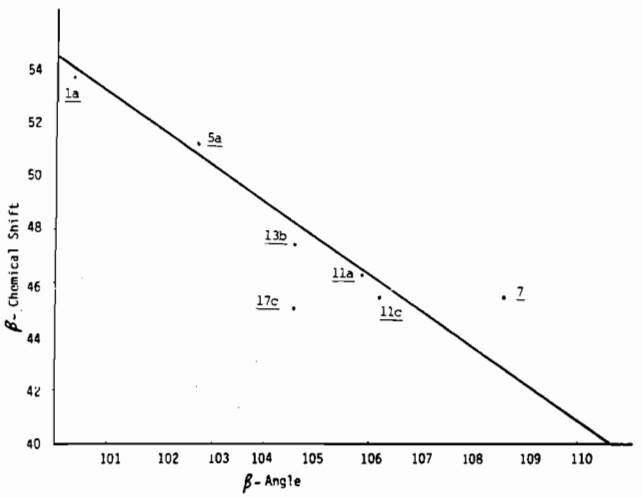

Figure 9. Graph of β angle vs. β chemical shift.

Experimental Section

All melting points were taken in capillary tubes with a Thomas-Hoover Uni-melt apparatus and are uncorrected. The ^1H and ^{13}C NMR spectra were determined on either a Bruker WP-200 or IBM-Bruker NR/80 NMR spectrometer in $CDCl_3$ solutions, except where noted, with Me_4Si (0.01%) and $CHCl_3$ as internal standards, respectively. Tris(2,4-pentanedione)chromium(III)[57] was added, in selected cases, to decrease the relaxation time (especially the quaternary carbons).[20] The 4000–200-cm^{-1} IR spectra were obtained on a Perkin-Elmer Model 983 infrared spectrophotometer connected to a Model 3600 infrared data station. The samples were prepared by mixing the ligand or complex (ca. 1 mg) with CsI (80–100 mg); then the micro cup sample holder containing the lightly compacted mixtures was placed in a Perkin-Elmer diffuse-reflectance accessory. The diffuse-reflectance spectral data were ratioed against a CsI blank. The function in the Kubelka–Munk equation ($F(R) = (1 - R)^2/2R$) provided a good approximation to the equivalent transmission spectrum. Other software used included ABEX (absorbance expansion), TAAT (transmittance–absorbance interconversion), and SMOOTH (Golay–Savitzky cubic function noise reduction). The peak parameter threshold was 3% T to exclude very small peaks.

Mass spectral (MS, 70 eV) data, herein reported as (assignment, relative intensity) were determined by D. Patterson on a Hewlett-Packard HP 5985 GC/mass spectrometer. The X-ray single-crystal data were obtained on an Enraf-Nonius CAD4 diffractometer equipped with Mo Kα radiation (λ = 0.71073 Å) and a graphite monochromator employing ω–2θ scans of variable rate. Scan rates were determined in a rapid prescan and were designed to yield approximately equal precision for all significant reflections. For monoclinic crystals, one quadrant of data was measured; for triclinic crystals, one hemisphere was measured. Crystal data, angular limits, and other experimental parameters are listed in Table VI. Absorption corrections were made by an empirical method based upon ψ scans of reflections near χ = 90°. Data reduction also included corrections for background, Lorentz, and polarization effects. Equivalent data were averaged and the data considered observed by the criterion in Table VI were used in refinements. All structures were solved

(56) Brubaker, G. R.; Johnson, D. W. *Inorg. Chem.* **1982**, *21*, 2223 and references cited therein.
(57) Fernelius, W. C.; Blanch, J. E. *Inorg. Synth.* **1957**, *5*, 130.

Table VII. Coordinates for 11c[a]

atom	x	y	z	atom	x	y	z
Pd	0.13947 (1)	0.44971 (5)	0.08594 (2)	C8	0.1657 (3)	0.6227 (7)	−0.1928 (4)
Cl	0.20766 (8)	0.5874 (2)	0.18133 (6)	C9	0.2142 (3)	0.6743 (7)	−0.1346 (4)
O1	0.3833 (3)	0.6017 (6)	−0.0747 (4)	C10	0.2108 (2)	0.6401 (6)	−0.0537 (3)
O2	0.3846 (2)	0.3907 (5)	−0.0046 (3)	C11	0.2629 (3)	0.7038 (7)	0.0084 (4)
O3	0.3732 (2)	0.7913 (8)	0.1163 (3)	C12	0.3174 (2)	0.5853 (7)	0.0414 (4)
O4	0.3971 (2)	0.5594 (6)	0.1601 (2)	C13	0.3635 (2)	0.5297 (9)	−0.0217 (3)
O5	0.1617 (2)	0.3305 (5)	0.3026 (2)	C14	0.3631 (3)	0.6565 (9)	0.1094 (5)
O6	0.0588 (2)	0.4443 (6)	0.2667 (3)	C15	0.4365 (3)	0.6059 (14)	0.2358 (4)
O7	0.1481 (1)	0.0579 (5)	0.1199 (2)	C16	0.4178 (4)	0.5740 (21)	0.2967 (6)
O8	0.2299 (2)	0.2065 (7)	0.1837 (2)	C17	0.4342 (3)	0.3253 (10)	−0.0549 (4)
N1	0.0668 (2)	0.3458 (5)	0.0145 (3)	C18	0.4579 (4)	0.1904 (16)	−0.0211 (7)
N2	0.1591 (2)	0.5468 (5)	−0.0317 (3)	C19	0.0343 (2)	0.2396 (7)	0.1379 (2)
C1	0.0224 (2)	0.2499 (7)	0.0483 (2)	C20	0.1099 (2)	0.2914 (7)	0.1693 (3)
C2	−0.0329 (2)	0.1829 (7)	0.0002 (3)	C21	0.1054 (3)	0.3668 (5)	0.2501 (3)
C3	−0.0425 (2)	0.2209 (7)	−0.0790 (3)	C22	0.1674 (3)	0.4112 (8)	0.3764 (3)
C4	0.0024 (2)	0.3250 (8)	−0.1124 (3)	C23	0.2355 (5)	0.3674 (11)	0.4192 (4)
C5	0.0576 (3)	0.3847 (6)	−0.0630 (3)	C24	0.1631 (2)	0.1726 (6)	0.1565 (3)
C6	0.1113 (2)	0.4907 (6)	−0.0910 (3)	C25	0.2833 (3)	0.0968 (7)	0.1691 (3)
C7	0.1141 (2)	0.5272 (9)	−0.1709 (3)	C26	0.3461 (5)	0.1518 (16)	0.2005 (13)

[a] Estimated standard deviations in the least significant digits are shown in parentheses.

Table VIII. Coordinates for 11a[a]

atom	x	y	z	atom	x	y	z
Pd	0.12769 (3)	0.11587 (1)	0.21240 (2)	C6	0.1897 (4)	−0.0059 (2)	0.0855 (3)
Cl	0.1266 (1)	0.23614 (5)	0.24336 (8)	C7	0.1941 (5)	−0.0775 (2)	0.0600 (3)
O1	0.0071 (4)	0.1635 (2)	0.4917 (2)	C8	0.1474 (6)	−0.1272 (2)	0.1347 (4)
O2	0.2542 (3)	0.1039 (1)	0.4599 (2)	C9	0.1020 (5)	−0.1057 (2)	0.2313 (3)
O3	−0.2632 (4)	0.0415 (2)	0.2852 (2)	C10	0.0980 (4)	−0.0335 (2)	0.2541 (3)
O4	−0.2368 (3)	0.1552 (1)	0.3383 (2)	C11	0.0614 (5)	−0.0003 (2)	0.3566 (3)
N1	0.2255 (4)	0.1203 (1)	0.0628 (2)	C12	0.0161 (4)	0.0802 (2)	0.3489 (2)
N2	0.1401 (3)	0.0144 (1)	0.1810 (2)	C13	0.0844 (5)	0.1220 (2)	0.4401 (3)
C1	0.2731 (5)	0.1780 (2)	0.0082 (3)	C14	0.3415 (5)	0.1393 (2)	0.5457 (3)
C2	0.3392 (5)	0.1726 (2)	−0.0907 (3)	C15	0.5092 (6)	0.1013 (3)	0.5685 (3)
C3	0.3532 (6)	0.1063 (2)	−0.1348 (3)	C16	−0.1746 (4)	0.0892 (2)	0.3219 (2)
C4	0.3040 (5)	0.0464 (2)	−0.0801 (3)	C17	−0.4082 (5)	0.1731 (2)	0.2925 (4)
C5	0.2419 (4)	0.0545 (2)	0.0183 (2)	C18	−0.3824 (6)	0.2045 (3)	0.1902 (4)

[a] Estimated standard deviations in the least significant digits are shown in parentheses.

by the heavy-atom method and refined by full-matrix least squares based upon F with weights $\sigma^{-2}(F_o)$, using the Enraf-Nonius SDP programs. Except where detailed below, non-hydrogen atoms were treated anisotropically, while hydrogen atoms were included as fixed contributions in calculated positions. Maximum densities in final difference maps, as well as R factors, are given in Table VI. Coordinates for non-hydrogen atoms for **11c**, **11a**, **11d**, **13b**, and **17c** are given in Tables VII–XI, respectively.

For the preparative thick-layer chromatography (ThLC), 2-mm silica gel PF-254-366 plates were used. Elemental analyses were performed by R. Seab in these laboratories.

Solvents. Anhydrous *N*,*N*-dimethylformamide (DMF) was purified to remove traces of HCN, which has been demonstrated to arise by its photolytic decomposition upon standing.[24] Anhydrous acetonitrile (MeCN) was prepared by distillation from CaH_2 and stored over molecular sieves.[58]

Reagents. Bipyridyl (**10a**), phenanthroline (**15a**), and 2,9-dimethylphenanthroline (**15b**) were purchased from Aldrich and recrystallized prior to use. 6-Methyl-2,2′-bipyridine (**10b**) was prepared by the addition of methyllithium to **10a**.[59] The α-chloromethyl heterocycles were prepared by the free-radical chlorination of the corresponding α-methyl heteroaromatic compounds by a standard *N*-chlorosuccinimide procedure.[22,23,60]

Stock complex solutions were made by dissolving the crystalline material in either EtOH or Me_2SO and diluted *immediately* before use with distilled H_2O. CsCl was obtained from Bethesda Research Laboratories. *E. coli* DNA polymerase I was purchased from Worthington Biochemicals. Radioisotopes were obtained from ICN. Schleicher and Schuell type BA-85 nitrocellulose filters were utilized in determining filter-binding events.

General Preparation of Ligands. A mixture of dialkyl malonate (4 equiv), the bis(chloromethyl) derivative (1 equiv), and anhydrous K_2CO_3 (3.5 equiv) in pure DMF was stirred at 25 °C for 24 h. The mixture was filtered and concentrated in vacuo to give a light yellow viscous oil, which was passed through a silica gel pad with CH_2Cl_2 and concentrated in vacuo, and the product was crystallized or rechromatographed (ThLC) on silica gel. Ligands previously prepared by this procedure, or a modification thereof, are referenced in the tables.

Diethyl α,α′-bis(ethoxycarbonyl)[2,2′-bipyridine]-6,6′-dipropanoate (10f) is a white crystalline solid, which was recrystallized from CH_2Cl_2/C_6H_{12}: yield 90%; mp 55–56 °C; ^{1}H NMR δ 1.22 (t, CH_2CH_3, J = 7.3 Hz), 3.45 (d, pyCH_2, J = 7.7 Hz), 4.15 (q, CH_2CH_3, J = 7.3 Hz), 4.22 (t, $CH(CO_2Et)_2$, J = 7.7 Hz), 7.18 (d, 5-py*H*, J = 7.7 Hz), 7.77 (t, 4-py*H*, J = 7.7 Hz), 8.24 (d, 3-py*H*, J = 7.7 Hz); ^{13}C NMR, Table IV; IR (KBr) 1742, 1726 (C=O), 1584, 1574, 1473, 1447 cm^{-1}; MS m/e 500 (M^+, 17), 455 ($M^+ - C_2H_5O$, 25), 427 ($M^+ - C_3H_5O_2$, 70), 335 (*100*). Anal. Calcd for $C_{26}H_{32}N_2O_8$: C, 62.39; H, 6.44; N, 5.60. Found: 62.42; H, 6.48; N, 5.43.

Ethyl α-(ethoxycarbonyl)[2,2′-bipyridine]-6-propanoate (10d) is an oil: bp 127–128 °C (0.6 mm); yield 94%; ^{1}H NMR δ 1.22 (t, CH_2CH_3, J = 7.3 Hz), 3.52 (d, pyCH_2, J = 7.3 Hz), 3.85 (t, $CH(CO_2Et)_2$, J = 7.3 Hz), 4.21 (m, CH_2CH_3), 7.20 (d, 5-py*H*, J = 7.9 Hz), 7.26 (dd, 5′-py*H*, $J_{4',5'}$ = 7.9 Hz, $J_{5',6'}$ = 4.3 Hz), 7.70 (t, 4′-py*H*, J = 7.9 Hz), 7.78 (t, 4-Py*H*, J = 7.9 Hz), 8.27 (d, 3-py*H*, J = 7.9 Hz), 8.45 (d, 3′-py*H*, J = 7.9 Hz), 8.64 (d, 6′-py*H*, J = 4.3 Hz); ^{13}C NMR, Table IV; IR (neat) 2980, 1730 (C=O), 1425, 1260 cm^{-1}; MS m/e 328 (M^+, 27), 255 ($M^+ - CO_2Et$, 83), 209 ($M^+ - C_5H_{11}O_3$, *100*), 183 ($M^+ - C_6H_9O_4$, 75). Anal. Calcd for $C_{18}H_{20}N_2O_4$: C, 65.84; H, 6.14; N, 8.53. Found: C, 65.72; H, 5.97; N, 8.49.

Ethyl α-(ethoxycarbonyl)(6-methyl-[2,2′-bipyridine])-6′-propanoate (10e) is an oil: bp 146–148 °C (1.3 mm); yield 91%; ^{1}H NMR δ 1.19 (t, CH_2CH_3, J = 7.3 Hz), 2.55 (s, pyCH_3), 3.50 (d, pyCH_2, J = 7.3 Hz), 4.19 (m, CH_2CH_3), 4.30 (t, $CH(CO_2Et)_2$, J = 7.3 Hz), 7.07 (d, 5-py*H*, J = 7.3 Hz), 7.14 (d, 5′-py*H*, J = 7.3 Hz), 7.62 (t, 4-py*H*, J = 7.3 Hz), 7.64 (t, 4′-py*H*, J = 7.3 Hz), 8.24 (d, 3-py*H*, J = 7.3 Hz), 8.28 (d, 3′-py*H*, J = 7.3 Hz); ^{13}C NMR, Table IV; MS m/e 342 (M^+, 25), 297

(58) Gordon, A. J.; Ford, R. A. "The Chemist's Companion"; Wiley: New York, 1972; p 431.
(59) Kaufmann, J.; Konig, J.; Woltermann, A. *Chem. Ber.* **1976**, *109*, 3864.
(60) Newkome, G. R.; Kiefer, G. E.; Puckett, W. E.; Vreeland, T. *J. Org. Chem.* **1983**, *48*, 5112.

Table IX. Coordinates for 11d[a]

atom	x	y	z	B, Å²	atom	x	y	z	B, Å²
Pd	0.4213 (1)	0.9584 (1)	0.16660 (9)		Pd′	0.8531 (1)	0.5066 (1)	0.13749 (9)	
O1	0.091 (1)	0.8125 (9)	−0.0363 (8)	7.3 (4)	O1′	1.170 (2)	0.452 (1)	0.2969 (13)	14.6 (7)
O2	−0.060 (1)	0.8658 (10)	0.0195 (9)	9.4 (5)	O2′	1.272 (2)	0.579 (2)	0.3867 (16)	18.5 (9)
O3	0.029 (1)	1.0656 (11)	0.1993 (10)	9.8 (5)	O3′	1.108 (2)	0.753 (1)	0.4208 (12)	13.3 (6)
O4	0.029 (1)	0.9366 (10)	0.2132 (9)	8.7 (4)	O4′	1.035 (2)	0.646 (1)	0.4599 (13)	15.3 (7)
O5	0.552 (1)	1.1104 (11)	0.3662 (9)	9.2 (4)	O5′	0.594 (1)	0.584 (1)	0.2356 (9)	8.6 (4)
O6	0.697 (1)	1.0440 (9)	0.3086 (8)	8.0 (4)	O6′	0.597 (1)	0.591 (1)	0.1106 (9)	10.0 (5)
O7	0.400 (1)	0.8455 (10)	0.2936 (9)	8.3 (4)	O7′	0.616 (2)	0.348 (1)	0.1564 (12)	13.1 (6)
O8	0.416 (1)	0.9914 (9)	0.3902 (8)	7.1 (4)	O8′	0.725 (1)	0.465 (1)	0.2629 (9)	9.3 (4)
O9	0.319 (1)	1.0375 (8)	0.2510 (7)		O9′	0.862 (1)	0.6200 (9)	0.2569 (7)	
O10	0.391 (1)	1.1601 (9)	0.2399 (9)		O10′	0.849 (1)	0.7184 (11)	0.2059 (10)	
N1	0.524 (1)	0.8798 (8)	0.0934 (7)	3.9 (3)	N1′	0.838 (1)	0.3971 (9)	0.0218 (9)	5.1 (4)
N2	0.352 (1)	0.9407 (8)	0.0379 (8)	4.0 (3)	N2′	1.030 (1)	0.4946 (10)	0.1167 (9)	5.4 (4)
C1	0.605 (1)	0.851 (1)	0.1296 (10)	4.5 (4)	C1′	0.730 (2)	0.356 (1)	−0.017 (1)	7.0 (6)
C2	0.689 (2)	0.803 (1)	0.0831 (10)	5.3 (5)	C2′	0.712 (2)	0.277 (1)	−0.103 (1)	6.9 (6)
C3	0.681 (2)	0.791 (1)	−0.0028 (11)	5.4 (5)	C3′	0.805 (2)	0.251 (1)	−0.138 (1)	7.0 (6)
C4	0.601 (2)	0.818 (1)	−0.0423 (10)	5.0 (5)	C4′	0.916 (2)	0.290 (1)	−0.101 (1)	6.6 (6)
C5	0.519 (2)	0.865 (1)	0.0100 (11)	4.6 (4)	C5′	0.931 (2)	0.370 (1)	−0.015 (1)	6.0 (5)
C6	0.425 (1)	0.897 (1)	−0.0238 (10)	4.1 (4)	C6′	1.037 (2)	0.421 (1)	0.036 (1)	5.3 (5)
C7	0.404 (1)	0.886 (1)	−0.1091 (9)	3.9 (4)	C7′	1.142 (2)	0.393 (1)	0.001 (1)	6.9 (6)
C8	0.312 (2)	0.919 (1)	−0.1317 (11)	5.5 (5)	C8′	1.239 (2)	0.450 (1)	0.060 (1)	6.9 (6)
C9	0.240 (2)	0.961 (1)	−0.0711 (11)	5.3 (5)	C9′	1.236 (2)	0.521 (1)	0.139 (1)	6.3 (5)
C10	0.260 (2)	0.970 (1)	0.0146 (10)	4.7 (4)	C10′	1.124 (2)	0.541 (1)	0.166 (1)	5.5 (5)
C11	0.180 (1)	1.011 (1)	0.0748 (10)	4.4 (4)	C11′	1.122 (2)	0.625 (1)	0.255 (1)	5.8 (5)
C12	0.122 (1)	0.941 (1)	0.1019 (10)	4.6 (4)	C12′	1.091 (2)	0.586 (1)	0.320 (1)	8.3 (6)
C13	0.047 (2)	0.871 (1)	0.0279 (12)	6.6 (5)	C13′	1.181 (3)	0.531 (2)	0.344 (2)	14.1 (11)
C14	0.055 (2)	0.991 (1)	0.1761 (13)	7.4 (6)	C14′	1.084 (2)	0.682 (2)	0.418 (2)	11.3 (9)
C15	−0.057 (2)	0.970 (2)	0.2810 (16)	10.5 (8)	C15′	1.027 (4)	0.746 (3)	0.555 (3)	19.9 (16)
C16	0.004 (3)	0.985 (2)	0.3593 (20)	15.3 (12)	C16′	1.000 (4)	0.690 (3)	0.589 (3)	22.2 (18)
C17	0.016 (2)	0.747 (2)	−0.1213 (15)	9.4 (7)	C17′	1.259 (3)	0.390 (3)	0.304 (2)	17.6 (13)
C18	0.084 (3)	0.706 (2)	−0.1821 (18)	13.2 (11)	C18′	1.344 (3)	0.391 (3)	0.255 (2)	18.0 (14)
C19	0.593 (2)	0.867 (1)	0.2202 (12)	6.1 (5)	C19′	0.638 (2)	0.402 (1)	0.026 (1)	8.0 (6)
C20	0.522 (2)	0.951 (1)	0.2691 (11)	5.1 (5)	C20′	0.684 (2)	0.472 (1)	0.128 (1)	6.1 (5)
C21	0.596 (2)	1.038 (1)	0.3165 (12)	6.8 (6)	C21′	0.618 (2)	0.547 (2)	0.154 (1)	9.5 (7)
C22	0.624 (3)	1.201 (2)	0.4282 (18)	13.0 (10)	C22′	0.547 (2)	0.671 (2)	0.273 (2)	10.4 (8)
C23	0.619 (3)	1.249 (2)	0.3912 (21)	16.0 (12)	C23′	0.525 (3)	0.691 (2)	0.363 (2)	12.4 (9)
C24	0.438 (2)	0.922 (1)	0.3168 (12)	6.2 (5)	C24′	0.672 (2)	0.421 (1)	0.184 (1)	7.2 (6)
C25	0.325 (2)	0.954 (2)	0.4303 (15)	9.6 (7)	C25′	0.700 (2)	0.422 (2)	0.323 (2)	12.1 (9)
C26	0.316 (2)	1.041 (2)	0.5097 (17)	11.4 (9)	C26′	0.761 (4)	0.494 (3)	0.403 (3)	20.1 (16)
C27	0.332 (2)	1.120 (1)	0.2724 (1)		C27′	0.851 (2)	0.691 (1)	0.260 (1)	
C28	0.280 (2)	1.186 (2)	0.3572 (9)		C28′	0.842 (2)	0.774 (2)	0.360 (2)	

[a] Estimated standard deviations in the least significant digits are shown in parentheses.

Table X. Coordinates for 13b[a]

atom	x	y	z	B, Å²	atom	x	y	z	B, Å²
Pd	0.84892 (7)	0.01446 (7)	0.17569 (7)	2.43 (2)	C9	0.8291 (9)	−0.2078 (10)	0.2349 (10)	3.9 (4)
O1	0.6681 (5)	0.0299 (6)	0.0905 (6)	3.9 (3)	C10	0.8229 (8)	−0.1301 (9)	0.2294 (9)	2.9 (4)
O2	0.7004 (6)	−0.0892 (7)	0.1096 (6)	4.0 (3)	C11	0.7757 (8)	−0.0808 (10)	0.2581 (9)	3.3 (4)
O3	0.7009 (6)	0.1040 (7)	0.2336 (6)	4.2 (3)	C12	0.7578 (7)	−0.0057 (9)	0.2107 (8)	2.6 (3)
O4	0.7831 (5)	0.0527 (6)	0.3325 (6)	3.3 (2)	C13	0.7046 (8)	−0.0176 (10)	0.1338 (9)	3.4 (3)
O5	0.8938 (7)	0.1956 (8)	0.2468 (7)	5.4 (3)	C14	0.7429 (8)	0.0552 (9)	0.2560 (9)	2.8 (3)
O6	0.7817 (6)	0.2062 (7)	0.1740 (7)	4.4 (3)	C15	0.6533 (9)	−0.1048 (11)	0.0299 (10)	4.3 (4)
O7	0.8391 (6)	0.0983 (7)	−0.0020 (7)	4.6 (3)	C16	0.6647 (11)	−0.1859 (12)	0.0149 (12)	5.6 (5)
O8	0.7487 (6)	0.1450 (6)	0.0277 (6)	3.8 (3)	C17	0.7701 (9)	0.1084 (10)	0.3839 (10)	3.9 (4)
N1	0.9350 (6)	−0.0020 (7)	0.1474 (6)	2.2 (2)	C18	0.8200 (10)	0.0974 (11)	0.4650 (10)	4.5 (4)
N2	0.8647 (6)	−0.0929 (7)	0.1984 (7)	2.4 (3)	C19	0.9370 (9)	0.1303 (10)	0.1380 (10)	3.5 (4)
C1	0.9673 (8)	0.0555 (9)	0.1272 (9)	2.5 (3)	C20	0.8596 (8)	0.1242 (9)	0.1340 (9)	2.8 (3)
C2	1.0262 (9)	0.0409 (10)	0.1032 (10)	3.9 (4)	C21	0.8370 (8)	0.1782 (9)	0.1832 (9)	3.4 (4)
C3	1.0449 (9)	−0.0306 (10)	0.1009 (10)	3.9 (4)	C22	0.8847 (11)	0.2488 (13)	0.3043 (12)	5.7 (5)
C4	1.0126 (8)	−0.0895 (9)	0.1215 (9)	3.0 (4)	C23	0.9291 (13)	0.3132 (14)	0.3070 (14)	7.3 (6)
C5	0.9547 (7)	−0.0727 (8)	0.1463 (8)	2.2 (3)	C24	0.8142 (8)	0.1211 (10)	0.0481 (9)	3.3 (4)
C6	0.9136 (8)	−0.1263 (9)	0.1747 (9)	2.8 (3)	C25	0.7084 (11)	0.1515 (12)	−0.0571 (12)	5.7 (5)
C7	0.9209 (9)	−0.2029 (10)	0.1788 (10)	3.5 (4)	C26	0.6748 (13)	0.0813 (14)	−0.0865 (14)	7.4 (6)
C8	0.8763 (9)	−0.2440 (10)	0.2088 (10)	3.8 (4)					
K	0.3326 (4)	0.1585 (4)	0.3940 (4)	9.8 (2)	O2S[b]	0.5540 (26)	0.0839 (29)	0.3342 (29)	14.3 (16)
O1A	0.4351 (9)	0.2338 (10)	0.3975 (10)	8.7 (5)	N1A	0.4604 (9)	0.237 (1)	0.469 (1)	5.8 (4)
O2A	0.5108 (8)	0.2743 (9)	0.5005 (9)	6.9 (4)	C1S	0.496 (3)	0.055 (3)	0.320 (3)	20 (2)
O3A	0.4256 (10)	0.2074 (12)	0.5068 (12)	10.9 (6)	C2S	0.489 (2)	0.020 (2)	0.378 (2)	13 (1)
O1S	0.5	0.0242 (22)	0.25	14.7 (11)					

[a] Estimated standard deviations in the least significant digits are shown in parentheses. [b] Population ½.

(M⁺ − OEt, 13), 269 (M⁺ − CO_2Et, *100*), 197 (M⁺ − $C_6H_9O_4$, 63). Anal. Calcd for $C_{19}H_{22}N_2O_4$: C, 66.65; H, 6.48; N, 8.18. Found: C, 66.36; H, 6.54; N, 8.02.

Dimethyl α,α′-bis(methoxycarbonyl)[1,10-phenanthroline]-2,9-dipropanoate (15c) is generated as white crystals: yield 100%; mp 120–122 °C; ^{1}H NMR δ 3.75 (s, CH_3), 3.75 (d, phenCH_2, J = 7.6 Hz), 4.66 (t,

Table XI. Coordinates for 17c[a]

atom	x	y	z	atom	x	y	z
Pd	0.18364 (6)	0.14296 (5)	0.21242 (3)	C11	0.7049 (7)	−0.3105 (6)	0.2694 (4)
Cl	−0.0170 (2)	0.3337 (2)	0.2612 (1)	C12	0.7092 (6)	−0.3307 (6)	0.2065 (4)
O1	−0.0246 (4)	0.4558 (5)	0.4176 (3)	C13	0.1935 (8)	0.0811 (7)	0.0774 (4)
O2	0.1447 (5)	0.5592 (5)	0.3665 (3)	C14	0.1182 (6)	0.2199 (6)	0.1165 (4)
O3	0.3412 (5)	0.2306 (7)	0.4798 (3)	C15	0.1888 (7)	0.1636 (8)	0.3873 (4)
O4	0.4756 (4)	0.3053 (5)	0.3890 (2)	C16	0.2358 (6)	0.3014 (6)	0.3755 (3)
O5	−0.1368 (6)	0.4071 (5)	0.0994 (3)	C17	0.0997 (7)	0.4457 (8)	0.3894 (4)
O6	−0.1158 (4)	0.1749 (5)	0.1443 (3)	C18	0.3576 (6)	0.2761 (7)	0.4202 (3)
O7	0.3222 (5)	0.2932 (6)	0.0572 (3)	C19	0.0409 (8)	0.7088 (7)	0.3800 (5)
O8	0.1221 (5)	0.4592 (5)	0.1126 (3)	C20	0.1045 (11)	0.7593 (10)	0.4259 (5)
N1	0.3445 (5)	−0.0196 (5)	0.1661 (3)	C21	0.0294 (13)	0.8033 (10)	0.3135 (6)
N2	0.3297 (4)	0.0175 (5)	0.2934 (2)	C22	0.5947 (8)	0.2988 (10)	0.4275 (4)
C1	0.3216 (5)	0.0356 (5)	0.3569 (3)	C23	0.7323 (8)	0.1589 (9)	0.4155 (5)
C2	0.4406 (7)	−0.0623 (8)	0.3958 (4)	C24	0.6239 (9)	0.4336 (9)	0.4087 (7)
C3	0.5634 (6)	−0.1744 (7)	0.3696 (3)	C25	−0.0595 (6)	0.2835 (6)	0.1199 (3)
C4	0.5767 (6)	−0.1975 (6)	0.3034 (4)	C26	−0.2814 (7)	0.2129 (8)	0.1468 (5)
C5	0.4556 (6)	−0.0998 (6)	0.2669 (3)	C27	−0.3038 (11)	0.1129 (13)	0.1115 (7)
C6	0.4649 (6)	−0.1186 (5)	0.1994 (3)	C28	−0.3506 (10)	0.2036 (16)	0.2160 (6)
C7	0.5876 (7)	−0.2317 (7)	0.1673 (4)	C29	0.1962 (6)	0.3279 (7)	0.0917 (3)
C8	0.5814 (6)	−0.2384 (6)	0.1008 (4)	C30	0.1935 (9)	0.5688 (9)	0.0961 (5)
C9	0.4624 (8)	−0.1387 (8)	0.0680 (4)	C31	0.0722 (11)	0.7143 (9)	0.0799 (7)
C10	0.3404 (6)	−0.0283 (5)	0.1023 (3)	C32	0.2608 (15)	0.5736 (14)	0.1459 (9)

[a] Estimated standard deviations in the least significant digits are given in parentheses.

C*H*$(CO_2Me)_2$, J = 7.6 Hz), 7.51 (d, 3,8-phen*H*, J = 8.6 Hz), 7.66 (s, 5,6-phen*H*), 8.10 (d, 4,7-phen*H*, J = 8.6 Hz); ^{13}C NMR, Table V; MS m/e 469 (M^+ + 1, 8), 468 (M^+, 27), 437 (22), 409 (*100*), 345 (87), 233 (61), 59 (98). Anal. Calcd for $C_{24}H_{24}N_2O_8$: C, 61.57; H, 5.13; N, 5.98. Found: C, 61.21; H, 5.31; N, 5.77.

Diethyl α,α′-bis(ethoxycarbonyl)[1,10-phenanthroline]-2,9-dipropanoate (15d) is formed as white crystals: yield 42%; mp 79–82 °C; ^1H NMR δ 1.22 (t, CH_2CH_3, J = 7.3 Hz), 3.74 (d, phenCH_2, J = 7.6 Hz), 4.21 (q, CH_2CH$_3$, J = 7.3 Hz), 4.58 (t, C*H*$(CO_2Et)_2$, J = 7.6 Hz), 7.53 (d, 3,8-phen*H*, J = 8.5 Hz), 7.67 (s, 5,6-phen*H*), 8.11 (d, 4,7-phen*H*, J = 8.5 Hz); IR (KBr) 2940, 1715 (C=O), 1600, 1580, 1480, 1355, 1250 cm^{-1}; MS m/e 525 (M^+ + 1, 6), 524 (M^+, 19), 480 (8.3), 479 (29), 451 (79), 359 (61), 233 (*100*), 219 (63). Anal. Calcd for $C_{28}H_{32}N_2O_8$: C, 64.11; H, 6.15; N, 5.34. Found: C, 63.99; H, 5.94; N, 5.20.

Diisopropyl α,α′-bis(isopropoxycarbonyl)[1,10-phenanthroline]-2,9-dipropanoate (15e) is formed as pale yellow crystals: yield 61%; mp 115–116 °C; ^1H NMR δ 1.18, 1.23 (2 d, $CH(CH_3)_2$, J = 6.3, 6.3 Hz), 3.72 (d, phenCH_2, J = 7.9 Hz), 4.44 (t, C*H*$(CO_2$-*i*-Pr$)_2$, J = 7.9 Hz), 5.04 (sep, C*H*$(CH_3)_2$, J = 6.3 Hz), 7.54 (d, 3,8-phen*H*, J = 8.5 Hz), 7.70 (s, 5,6-phen*H*), 8.12 (d, 4,7-phen*H*, J = 8.5 Hz); IR (KBr) 2965, 2920, 1715 (C=O), 1600, 1580, 1480, 1355 cm^{-1}; ^{13}C NMR, Table V; MS m/e 582 (M^+ + 2, 1), 581 (M^+ + 1, 2), 580 (M^+, 6), 234 (35), 233 (95), 231 (44), 43 (*100*). Anal. Calcd for $C_{32}H_{40}N_2O_8$: C, 66.20; H, 6.94; N, 4.83. Found: C, 65.95; H, 7.02; N, 4.93.

Preparation of Dichloropalladium(II) Complexes. Dichloro(6-methyl-2,2′-bipyridine)palladium(II) (9b). To a MeCN solution (50 mL) of $PdCl_2$ (1 mmol) was added 6′-methyl-2,2′-bipyridine (**10b**, 1 mmol) dissolved in MeCN (5 mL). The reaction was conducted under nitrogen, and after initial combination at 50 °C, the stirred solution was maintained at 25 °C for 2 h. The resultant precipitate was filtered, washed with MeCN, and dried in vacuo to give the orange solid: yield 90%; mp 249–252 °C dec; ^1H NMR δ 3.15 (s, pyCH_3), 7.37 (dd, 5′-py*H*, J = 6.0, 1.0 Hz), 7.48 (dd, 5-pyH, J = 6.0 Hz), 7.92–8.12 (m, 4,4′,3,3′-py*H*), 9.35 (d, 6-py*H*, J = 6.0 Hz); IR (CsI) 1590, 1480, 1240, 325 cm^{-1}.

Dichloro[diethyl α,α′-bis(ethoxycarbonyl)(2,2′-bipyridine)-6,6′-dipropanoate]palladium(II) (9d) was similarly prepared from **10f** and Li_2PdCl_4: yield 70%; mp 145–148 °C dec; ^1H NMR δ 1.19 (t, CH_2CH_3, J = 7.0 Hz), 4.11 (q, CH_2CH$_3$, J = 7.0 Hz), 4.12 (d, pyCH_2CH, J = 7.0 Hz), 4.51 (t, pyCH_2C*H*, J = 7.0 Hz), 7.24 (dd, 5-py*H*, J = 7.8, 1.0 Hz), 7.90 (t, 4-py*H*, J = 7.8 Hz), 8.28 (dd, 3-py*H*, J = 7.8, 1.0 Hz).

Dichloro[dimethyl α,α′-bis(methoxycarbonyl)(1,10-phenanthroline)-2,9-dipropanoate]palladium(II) (16c) was prepared as dark orange crystals: yield 100%; mp 212 °C dec; ^1H NMR δ 3.70 (s, CH_3), 4.36 (d, phenCH_2, J = 7.6 Hz), 4.85 (t, phenCH_2C*H*, J = 7.6 Hz), 7.62 (d, 3,8-phen*H*, J = 8.3 Hz), 7.88 (s, 5,6-phen*H*), 8.38 (d, 4,7-phen*H*, J = 8.3 Hz). Anal. Calcd for $C_{24}H_{24}N_2O_8PdCl_2$: C, 44.64; H, 3.75; N, 4.34. Found: C, 44.39; H, 3.92; N, 4.29.

General Preparation of *cis*-(Bipyridine)Palladium Complexes. Method A. An alcoholic solution of NaOR or KOR (2.5 equiv) was added dropwise to an anhydrous THF solution of $PdCl_2(PhCN)_2$ or Na_2PdCl_4 (1.0 equiv) and the ligand (1.0 equiv). The mixture was stirred for 24 h at 25 °C and then concentrated in vacuo to give the crude complex, which was recrystallized or chromatographed (ThLC on silica gel, HPLC) to afford the pure complex.

Method B. A mixture of Na_2PdCl_4 or $PdCl_2$ (1.5 equiv) and the ligand (1.0 equiv) in anhydrous MeCN was stirred for 1 h at 50 °C. Anhydrous K_2CO_3 (3.0 equiv) was added and the reaction mixture stirred for 24 h at 55 °C under a nitrogen atmosphere. $AgNO_3$ (2 equiv) was added and the mixture stirred for 2 h at 50 °C. The heterogeneous mixture was filtered through Celite and concentrated, whereupon the crude product was passed through a silica gel pad (eluent CH_2Cl_2) and concentrated in vacuo to give the product, which was recrystallized or chromatographed (ThLC, silica gel; HPLC).

[[2,2′-Bipyridine]-6,6′-diylbis[1,1-bis(methoxycarbonyl)-2,1-ethanediyl]-*C*,*C*′,*N*,*N*′]palladium (13a) was prepared by Method A and recrystallized from $CHCl_3/C_6H_{12}$ to give a yellow powder: yield 48%; mp 178–182 °C dec; ^1H NMR δ 3.77 (s, OCH_3), 4.02 (s, pyCH_2), 7.50 (d, 5-py*H*, J = 8.0 Hz), 7.62 (d, 3-py*H*, J = 8.0 Hz), 7.89 (t, 4-py*H*, J = 8.0 Hz); IR (KBr) 1730 (C=O), 1290, 1190, 1065 cm^{-1}; MS m/e 548 (M^+, 5), 547 (M^+ − 1, 5), 351, 325, 321, 293 (*100*). Anal. Calcd for $C_{22}H_{22}N_2O_8Pd$: C, 48.15; H, 4.04; N, 5.10. Found: C, 48.18; H, 4.25; N, 4.99.

[[2,2′-Bipyridine]-6,6′-diylbis[1,1-bis(ethoxycarbonyl)-2,1-ethanediyl]-*C*,*C*′,*N*,*N*′]palladium (13b) was prepared by method A and recrystallized from C_6H_6/Et_2O to afford (25%) yellow crystalline needles. The complex was also prepared by method B and recrystallized from CH_2Cl_2/C_6H_{12} to give yellow crystalline needles identical in all respects with those prepared by method A: yield 90%; mp 220–222 °C dec (in air); ^1H NMR (CD_2Cl_2) δ 1.21 (t, CH_2CH_3, J = 7.2 Hz), 3.90 (s, pyCH_2), 4.14 (m, CH_2CH$_3$), 7.49 (d, 5-py*H*, J = 7.8 Hz), 7.64 (d, 3-py*H*, J = 7.8 Hz), 7.91 (t, 4-py*H*, J = 7.8 Hz); MS m/e 606 (M^+ (^{108}Pd), 2.4), 603 (M^+ (^{105}Pd), 2.0), 561 and 558 ($M^+ - C_2H_5O$, 1.2), 205 (*100*). Anal. Calcd for $C_{26}H_{30}N_2O_8Pd$: C, 51.62; H, 5.00; N, 4.63. Found: C, 51.65; H, 5.05; N, 4.60.

[[2,2′-Bipyridine]-6,6′-diylbis[1,1-bis((1-metbyletboxy)carbonyl)-2,1-ethanediyl]-*C*,*C*′,*N*,*N*′]palladium (13c) was prepared by method B and recrystallized from CH_2Cl_2/C_6H_{12} to afford (70%) yellow crystals: mp 130–104 °C dec; ^1H NMR δ 1.02, 1.13 (2 d, $(CH^A_3)(CH^B_3)$CH, J = 6.2, 6.2 Hz), 3.88 (s, pyCH_2), 4.94 (sep, C*H*, J = 6.2 Hz), 7.46 (dd, 5-py*H*, J = 5.5, 3.6 Hz), 7.89 (dd, 3-py*H*, J = 5.5, 3.6 Hz), 8.00 (t, 4-py*H*, J = 5.5 Hz); IR (KBr) 1725 (C=O), 1380, 1365 cm^{-1}.

Chloro[2-ethoxy-1-(ethoxycarbonyl)-1-[[6-[3-etboxy-2-(etboxycarbonyl)-3-oxopropyl][2,2′-bipyridine]-6′-yl]methyl]-2-oxoethyl-*C*,*N*,*N*′]palladium (11c) was prepared by method B without added $AgNO_3$ and recrystallized from CH_2Cl_2/C_6H_{12} or chromatographed on silica gel with C_6H_6 elution to give (90%) a yellow powder: mp 187–189 °C dec; ^1H NMR (CD_2Cl_2) δ 1.18, 1.26 (2 t, CH_2CH_3, J = 7.3 Hz), 3.59 (s, pyCH_2), 3.93 (d, pyCH_2CH, J = 7.8 Hz), 4.11 (dq, $CH(CO_2CH_2CH_3)_2$, J = 7.1, 1.0 Hz), 4.15 (dq, $PdC(CO_2CH_2CH_3)_2$, J = 7.1, 7.3 Hz), 4.25, 4.29 (2 d, pyCH_2C*H*, J = 8.5, 8.5 Hz), 7.39 (dd, 5-py*H*, J = 6.4, 2.7 Hz), 7.54 (dd, 5′-py*H*, J = 7.8, 1.0 Hz, 7.77 (dd, 3′-py*H*, J = 7.6, 1.0 Hz), 7.90 (dd, 3-py*H*, J = 5.9, 1.5 Hz), 7.91 (t, 4′-py*H*, J = 7.9 Hz), 7.96 (t, 4-py*H*, J = 8.0 Hz); IR (KBr) 1728 (C=O), 1604, 1573, 1473,

1445 cm^{-1}. Anal. Calcd for $C_{26}H_{31}N_2O_8PdCl$: C, 50.91; H, 5.09; N, 4.57. Found: C, 50.81; H, 4.95; N, 4.40.

(Acetato)[2-ethoxy-1-(ethoxycarbonyl)-1-[[6-[3-ethoxy-2-(ethoxycarbonyl)-3-oxopropyl][2,2′-bipyridine]-6′-yl]methyl]-2-oxoethyl-*C,N,N′*]palladium (11d). To a solution of **11c** (25 mg) in MeCN was added excess AgOAc and the mixture stirred for 2 h at 25 °C. The mixture was filtered (Celite) and concentrated in vacuo to dryness to afford a yellow powder, which was recrystallized from CH_2Cl_2/C_6H_{12} to give **11d**, as yellow microneedles: yield 95%; mp 194–197 °C dec; ^1H NMR δ 1.18, 1.36 (2 t, CH_2CH_3, J = 7.1 Hz), 1.96 (s, $COCH_3$), 3.33 (d, pyCH_2, J = 8.0 Hz), 3.65 (s, pyCH_2), 4.12, 4.20 (2 dq, CH_2CH_3, J = 7.3, 3.0 Hz), 4.44 (t, CH_2CH, J = 8.0 Hz), 7.02 (dd, 5-py$H$, J = 6.1, 1.4 Hz), 7.28 (dd, 5′-py$H$, J = 7.2, 1.6 Hz), 7.80 (t, 4′-py$H$, J = 7.2 Hz), 7.97 (dd, 3′-py$H$, J = 7.2, 1.6 Hz), 7.99 (t, 4-py$H$, J = 7.9 Hz), 8.21 (dd, 3-py$H$, J = 7.9, 1.4 Hz); IR (KBr) 1730 (C=O), 1630, 1320 cm^{-1}.

Chloro[2-ethoxy-1-(ethoxycarbonyl)-1-[[[2,2′-bipyridine]-6′-yl]methyl]-2-oxoethyl-*C,N,N′*]palladium (11a) was prepared as yellow needles: mp 183–186 °C dec; yield 60%; ^1H NMR δ 1.32 (t, CH_2CH_3, J = 7.3 Hz), 3.83 (s, pyCH_2), 4.27 (m, CH_2CH_3), 7.44 (d, 5,5′-py$H$, J = 5.5 Hz), 7.84 (t, 4-py$H$, J = 5.5 Hz), 7.93 (t, 4′-py$H$, J = 5.5 Hz), 8.02 (d, 3,3′-py$H$, J = 5.5 Hz), 8.81 (d, 6-py$H$, J = 5.5 Hz); IR (CsI) 2985, 1700 (C=O), 1480, 1270 cm^{-1}; MS m/e 411 ((M^+ + 1) − 2 Et, 2), 281 ($M^+ - C_6H_6OPdCl$, 25), 255 ($M^+ - C_3H_4O2PdCl$, 36), 236 ($M^+ - C_4H_{11}O_2PdCl$, *100*), 209 ($M^+ - C_5H_{10}O_3PdCl$, 53). Anal. Calcd for $C_{18}H_{19}N_2O_4PdCl$: C, 46.08; H, 4.08; N, 5.97. Found: C, 45.97; H, 4.08; N, 5.94.

Chloro[2-ethoxy-1-(ethoxycarbonyl)-1-[[[6-methyl][2,2′-bipyridine]-6′-yl]methyl]-2-oxoethyl-*C,N,N′*]palladium (11b) was prepared as yellow needles: mp 219–221 °C dec; yield 82%; ^1H NMR δ 1.29 (t, CH_2CH_3, J = 7.3 Hz), 2.98 (s, pyCH_3), 3.62 (s, pyCH_2), 4.25 (m, CH_2CH_3), 7.33 (dd, 5-py$H$, $J_{4,5}$ = 7.4 Hz, $J_{3,5}$ = 1.8 Hz), 7.50 (d, 5′-py$H$, J = 7.8 Hz), 7.75 (2 d, 3′-py$H$, J = 7.8 Hz; 3-py$H$, J = 7.4 Hz), 7.88 (t, 4-py$H$, J = 7.4 Hz), 7.92 (t, 4′-py$H$, J = 7.8 Hz); MS m/e 484 (M^+ (^{37}Cl), 1), 482 (M^+ (^{35}Cl), 1) 296 ($M^+ - C_2H_5OPdCl$, 37), 250 ($M^+ - C_4H_{11}O_2PdCl$, *100*), 222 ($M^+ - C_5H_{11}O_2PdCl$, 48). Anal. Calcd for $C_{19}H_{21}N_2O_4PdCl$: C, 47.22; H, 4.38; N, 5.80. Found: C, 46.99; H, 4.40;, N, 5.74.

Chloro[2-methoxy-1-(methoxycarbonyl)-1-[[9-[3-methoxy-2-(methoxycarbonyl)-3-oxopropyl][1,10-phenanthroline]-2-yl]methyl]-2-oxoethyl-*C,N,N′*]palladium (17a) was obtained as yellow crystals: yield 50%; mp 120–122 °C dec; ^1H NMR δ 3.70, 3.84 (2 s, CH_3), 3.86 (s, phenCH_2), 4.11 (d, phenCH_2CH, J = 8.0 Hz), 4.39 (t, phenCH_2CH, J = 8.0 Hz), 7.65 (d, 8-phen$H$, J = 6.5 Hz), 7.80 (d, 3-phen$H$, J = 6.5 Hz), 7.89 (s, 5,6-phen$H$), 8.36 (d, 7-phen$H$, J = 6.5 Hz), 8.43 (d, 4-phen$H$, J = 6.5 Hz); MS m/e 466 (3), 436 (3), 435 (9), 434 (4), 422 (25), 407 (28), 375 (93), 349 (54), 317 (*100*), 44 (66). Anal. Calcd for $C_{24}H_{23}N_2O_8PdCl$: C, 47.24; H, 3.96; N, 4.59. Found: C, 47.11; H, 4.01; N, 4.52.

Chloro[2-ethoxy-1-(ethoxycarbonyl)-1-[[9-[3-ethoxy-2-(ethoxycarbonyl)-3-oxopropyl][1,10-phenanthroline]-2-yl]methyl]-2-oxoethyl-*C,N,N′*]palladium (17b) was obtained as yellowed crystals: yield 50%; mp 194–195 °C dec; ^1H NMR δ 1.15, 1.31 (2 t, CH_2CH_3, J = 6.7 Hz), 3.79 (s, phenCH_2), 4.01 (d, phenCH_2CH, J = 7.3 Hz), 4.09, 4.25 (2 q, CH_2CH_3, J = 6.7 Hz), 4.34 (t, phenCH_2CH, J = 7.4 Hz), 7.56 (d, 8-phen$H$, J = 8.5 Hz) 7.74 (d, 3-phen$H$, J = 8.5 Hz), 7.85 (s, 5,6-phen$H$), 8.33 (d, 7-phen$H$, J = 8.5 Hz), 8.38 (d, 4-phen$H$, J = 8.5 Hz). Anal. Calcd for $C_{28}H_{31}N_2O_8PdCl$: C, 50.54; H, 4.70; N, 4.21. Found: C, 50.05; H, 4.86; N, 4.59.

Chloro[2-(1-methylethoxy)-1-((1-methylethoxy)carbonyl)-1-[[9-[3-(1-methylethoxy)-2-((1-methylethoxy)carbonyl)-3-oxopropyl][1,10-phenanthroline]-2-yl]methyl]-2-oxoethyl-*C,N,N′*]palladium (17c) was obtained as yellow crystals: yield 86%; mp 88–92 °C; ^1H NMR δ 1.14, 1.19 (2 d, $(CH_3)_2CH$, J = 6.1, 6.1 Hz), 1.28, 1.35 (2 d, $(CH_3)_2CH$, J = 6.1, 6.1 Hz), 3.81 (s, phenCH_2), 4.10 (d, phenCH_2, J = 8.0 Hz), 4.43 (t, phenCH_2CH, J = 8.0 Hz), 4.98, 5.13 (2 sep, $(CH_3)_2CH$, J = 6.1 Hz), 7.67 (d, 8-phen$H$, J = 8.5 Hz), 7.79 (d, 3-phen$H$, J = 8.5 Hz), 7.86 (s, 5,6-phen$H$), 8.31 (d, 7-phen$H$, J = 8.5 Hz), 8.37 (d, 4-phen$H$, J = 8.5 Hz); IR (KBr) 2985, 1715 (C=O), 1590, 1495, 1460, 1370, 1265 cm^{-1}; MS m/e 684 (2), 520 (22), 519 (22), 518 (18), 491 (26), 232 (68), 231 (72), 229 (89), 43 (*100*). Anal. Calcd for $C_{32}H_{39}N_2O_8PdCl$: C, 53.27; H, 5.41; N, 3.88. Found: C, 53.66; H, 5.63; N, 3.79.

X-ray Experiments. Peculiarities of individual refinements are described below.

11a and **17c**: None.

11c: The large thermal parameters of C26, the terminal carbon atom of an ethyl ester, is likely indicative of disorder, but partially occupied positions are not sufficiently resolved to allow their individual refinement. This atom was treated as a single position for least-squares purposes.

11d: The relatively weak scattering of the crystals and the large number of potentially refineable parameters (two independent molecules) prohibited full anisotropic refinement. Hydrogen atoms were ignored. Thus only the Pd atoms and those of the acetate ligand, the identity of which was initially in question, were treated in that fashion. The acetate was unambiguously identified by refinements with different scattering factors and examination of bond distances.

13b: Due to the tiny size of the crystals and limited data set, only the isotropic refinement was carried out. In addition to the 1 mol of KNO_3/mol of **13b** in the crystal, $^1/_2$ mol of EtOAc was located, disordered across a twofold axis. The ester oxygen atom (O1S) lies on the axis, while the carbon atoms of the ethyl and acetate groups approximately coincide, leading to two fully occupied carbon atoms in general positions. The carbonyl oxygen atom O2S lies in a half-occupied general position. This model was successful for solvent refinement, and hydrogen atoms of this group were ignored.

Biochemical Experiments. The preparation of phage PM2 [^{3}H]DNA has been described.[61] The resulting thymidine-labeled DNA had a specific activity of 156 cpm/fmol of DNA molecules.

Analysis of Filter-Binding Events. Reaction mixtures (0.05 mL) contained PM2 DNA molecules (50–70 fmol), Tris-HCl (25 mM, pH 7.5), $MgCl_2$ (10 mM), and the specific Pd complex. Incubations were at 37 °C for 5 min. The reactions were terminated by the addition of sodium dodecyl sulfate (0.15 mL, 0.01%) and EDTA (2.5 mM). Single-strand breaks were analyzed as previously described.[61] Associative binding of the complex to DNA was determined similarly except that distilled H_2O (0.3 mL) was added instead of alkali and acid. A filter-binding event is that amount of DNA *retained* on the nitrocellulose filter in the presence of the metal complex.

Buoyant Density Determination. Incubation conditions were as described above for analysis of filter-binding events. After termination of the reaction, unlabeled PM2 DNA (260 fmol) was added, as a carrier. Polyallomer centrifuge tubes were filled to 3.0 mL with the reaction mixture suspended in CsCl (density 1.70 g/mL). The tubes were topped with mineral oil and centrifuged at 44 000 rpm for 24 h at 24 °C in a SW 50.1 rotor. Fractions (0.08 mL) were collected from the bottom of the tube, and the refractive index was determined immediately with an Abbe refractometer. Each aliquot was diluted with distilled water (0.3 mL) and aqueous fluor (3.5 mL). The results are expressed as percentage of recovered counts per fraction. Average recovery of radioactivity from the gradient was 71%.

DNA Synthesis. Reaction mixtures (0.05 mL) contained K_3PO_4 (70 mM, pH 7.5), Tris-HCl (25 mM, pH 7.5), $MgCl_2$ (10 mM), dTTP (100 μM), dCTP (100 μM), dGTP (100 μM), [α-^{3}H]dATP (1.2 μM, 17 Ci/mmol), PM2 DNA (80 fmol), *E. coli* DNA polymerase I (0.15 units), and complex **13b**. Following incubation of **13b** with DNA in Tris-HCl (25 mM, pH 7.5), $MgCl_2$ (10 mM), *E. coli* DNA polymerase I in K_3PO_4 (70 mM, pH 7.5), and labeled dNTPs were added and incubated at 37 °C for 1 h. The reaction was terminated by cooling on ice for 15 min and adding Cl_3AcOH (0.15 mL, 10%). The acid-insoluble product was collected on Whatman GF/C filters soaked in Cl_3AcOH (10%). Each filter was washed with Cl_3AcOH (10%, 30 mL), dried, and counted to determine radioactivity.

Acknowledgment. We wish to thank the National Science Foundation and the LSU Center for Energy Studies for partial support of this research.

Registry No. 5b, 94570-66-8; **9b**, 80822-41-9; **9d**, 80822-40-8; **10a**, 366-18-7; **10b**, 56100-22-2; **10d**, 83478-65-3; **10e**, 83478-66-4; **10f**, 74509-77-6; **10** (R = R′ = CH_2Cl), 74065-64-8; **10** (R = R′ = $CH_2CH(CO_2Me)_2$), 87518-62-5; **10** (R = R′ = $CH_2CH(CO_2Pr\text{-}i)_2$),

(61) Kuhnlein, U.; Tsang, S. S.; Edwards, J. J. *Mutat. Res.* **1979**, *64*, 167.
(62) Newkome, G. R.; Gupta, V. K.; Fronczek, F. R. *Inorg. Chem.* **1983**, *22*, 171.
(63) Newkome, G. R.; Puckett, W. E.; Gupta, V. K.; Fronczek, F. R. *Organometallics* **1983**, *2*, 1247.
(64) Gupta, V. K., unpublished results, 1983.
(65) Newkome, G. R.; Kawato, T. *Inorg. Chim. Acta* **1979**, *37*, L481. Newkome, G. R.; Kawato, T.; Kohli, D. K.; Puckett, W. E.; Oliver, B. D.; Chiari, G.; Fronczek, F. R.; Deutsch, W. A. *J. Am. Chem. Soc.* **1981**, *103*, 3423. Newkome, G. R.; Kohli, D. K.; Fronczek, F. R. *J. Am. Chem. Soc.* **1982**, *104*, 994.
(66) Newkome, G. R.; Gupta, V. K. *Inorg. Chim. Acta* **1982**, *65*, L165.
(67) Newkome, G. R.; Pantaleo, D. C.; Puckett, W. E.; Ziefle, P. L.; Deutsch, W. A. *J. Inorg.* Nucl. *Chem.* **1981**, *43*, 1529.
(68) Livingstone, S. E. *J. Proc. R. Soc. N. S. W.* **1952**, *86*, 32.
(69) Newkome, G. R.; Kiefer, G. E.; Gupta, V. K.; Fronczek, F. R.; Xia, Y., to be submitted for publication in *Inorg. Chem.*
(70) Newkome, G. R.; Kiefer, G. E.; Fronczek, F. R.; Watkins, S. F., to be submitted for publication in *Acta Crystallogr., Sect. C: Cryst. Struct. Commun.*

94537-99-2; **11a**, 94570-75-9; **11b**, 94570-67-9; **11c**, 74468-76-1; **11d**, 94570-68-0; **13a**, 94570-69-1; **13b**, 74468-77-2; **13c**, 94570-70-4; **15a**, 66-71-7; **15c**, 94537-96-9; **15d**, 94537-97-0; **15e**, 94537-98-1; **15** (R = CH_2Cl), 87518-61-4; **16c**, 94570-71-5; **17a**, 94570-72-6; **17b**, 94570-73-7; **17c**, 94570-74-8; $CH_2(CO_2Me)_2$, 108-59-8; $CH_2(CO_2Et)_2$, 105-53-3; $CH_2(COPr\text{-}i)_2$, 13195-64-7; $PdCl_2$, 7647-10-1; Li_2PdCl_4, 15525-45-8; $PdCl_2(PhCN)_2$, 14220-64-5; Na_2PdCl_4, 13820-53-6; EtONa, 141-52-6.

Supplementary Material Available: Tables of IR frequencies of pyridine-, pyrazine-, 2,2'-bipyridine-, and 1,10-phenanthroline-based ligands and their complexes, coordinates of H atoms for complexes **11a**, **11d**, **13b**, and **17c**, bond distances and angles for **11a**, **11c**, **11d**, **13b**, and **17c**, anisotropic thermal parameters for complexes **11a**, **11c**, **11d**, and **17c**, and structure factors for **11a**, **11c**, **11d**, **13b**, and **17c** (98 pages). Ordering information is given on any current masthead page.

Contribution from the Department of Chemistry,
University of Virginia, Charlottesville, Virginia 22901

Carbon-Rich Metallacarboranes. 13.[1] Synthesis and Structure of Bis(carboranyl)cobalt Complexes Derived from $(C_2H_5)_4C_4B_8H_8^{2-}$

ZHU-TING WANG,[2] EKK SINN, and RUSSELL N. GRIMES*

Received June 26, 1984

The reaction of $CoCl_2$ with $Et_4C_4B_8H_8^{2-}$ ion in tetrahydrofuran produced two crystalline dicobalt complexes that were isolated by column and plate chromatography: red $(Et_4C_4B_8H_8)_2Co_2$ (**1**), 35% yield, and red-orange paramagnetic $(Et_4C_4B_8H_7)_2Co_2$ (**2a**), 15%. From two-dimensional (2D) ^{11}B-^{11}B NMR data, **1** is proposed to consist of a pair of 14-vertex *closo*-$Co_2C_4B_8$ polyhedra sharing a common Co-Co edge, a previously unknown geometry in metallacarborane chemistry. Electron pairing between the formal Co(II) centers is proposed to account for the observed diamagnetism. The same reaction, when followed by addition of $B_5H_8^-$ ion, generates several isolable complexes, including **1** (18%) and the minor products **2b** (an isomer of **2a**), $(Et_4C_4B_8H_8)$-$Co(Et_4C_4B_8H_7OC_4H_8)$ (**3a**), $(Et_4C_4B_8H_7)_2CoH$ (**4a**), and $(Et_4C_4B_4H_6)CoH(Et_4C_4B_8H_8)$ (**5**). Compound **2b** slowly rearranges at room temperature to an isomer, **2c**. Treatment of **1** with I_2 in acetone at 25 °C produces $(Et_4C_4B_8H_7)_2(OCMe_2)_2CoH$ (**3c**, 22%), isomers of $(Et_4C_4B_8H_7)_2(OH)Co$ (**3d**, 8%; **3e**, 9%), $(Et_4C_4B_8H_6OH)_2HCo$ (**3f**, 11%), and **2b** (19%). Products **2a**, **2b**, **2c**, and **4a** are proposed to have a direct B-B linkage between their carborane ligands. An X-ray crystallographic study of **3c** revealed that the carborane ligands are bridged by an acetone molecule via a B-O-B array in which the direct interligand boron-boron distance is 2.26 Å, considered weakly bonding. The second acetone is coordinated to a single boron atom on one of the cages, and the metal-bonded faces of the carborane ligands are inclined with a dihedral angle of 27.1°. The established and proposed structures are discussed in light of current cluster bonding theory, and implications concerning metal-promoted ligand fusion and coupling processes are considered. Crystal data: $[(C_2H_5)_4C_4B_8H_7]_2[OC(CH_3)_2]_2CoH$, $M_r = 692$, space group $P2_1/c$, $a = 9.897$ (7) Å, $b = 12.316$ (3) Å, $c = 33.31$ (2) Å, $\beta = 92.35$ (3)°, $V = 4057$ Å^3, $Z = 4$, $R = 0.073$ for 3054 reflections having $F_o^2 > 3\sigma(F_o^2)$.

Introduction

This series of papers is concerned with the structural and chemical consequences of high carbon content in polyhedral boron clusters. Formal replacement of boron by carbon in a borane framework increases the number of skeletal bonding electrons and hence, according to the polyhedral skeletal electron pair theory[3] (PSEPT), should lead to progressively more open cage geometry as the carbon/boron ratio increases, provided the framework composition is otherwise unchanged. Thus, $C_2B_{10}H_{12}$ with 26 skeletal electrons is a closed icosahedral cage; $C_4B_8H_{12}$ and its *C*-alkyl derivatives, with 28 electrons, are formally of the nido class and adopt open-cage geometries (but are fluxional in solution[4]). The $R_4C_4B_8H_8^{2-}$ dianions are 30-electron arachno systems whose geometries are still more open than the nido species, as deduced from X-ray structure determinations on a cobaltocenium derivative of $(CH_3)_4C_4B_8H_9^-$ and on several transition-metal π complexes of $R_4C_4B_8H_8^{2-}$ ligands.[4a,5]

While this general trend is in line with expectation from theory, the observed structures are often surprising and lend new insights into cluster bonding that are obtainable, at present, only through experiment—that is, via synthesis and structural characterization of specific compounds. Earlier reports from this laboratory[4a] have described the preparation and structures of a number of 11-14-vertex four-carbon metallocarboranes containing ML_n units, where M is Fe, Co, or Ni and L is an exo-polyhedral ligand such as C_5H_5. The present study was directed to bis(carboranyl)metal "commo"-type complexes, which contain two distinct metallacarborane cage systems joined at a common vertex. Species of this class whose carborane moiety is $R_2C_2B_4H_4^{2-}$ (R = alkyl), e.g., $H_2Fe(R_2C_2B_4H_4)_2$, undergo oxidative ligand fusion to form $R_4C_4B_8H_8$ carboranes;[4a,b] hence, it was of interest to determine if fusion could be similarly effected when one or both ligands is $R_4C_4B_8H_8^{2-}$.

In this paper we describe the synthesis and structural investigation of homo bis(carboranyl) complexes in which both ligands are C_4B_8 units; hetero-type species incorporating two different carborane systems are reported in the accompanying article.[6]

Results and Discussion

Reaction of $Et_4C_4B_8H_8^{2-}$ Ion with $CoCl_2$. The room-temperature interaction of a THF solution of $Na^+{}_2Et_4C_4B_8H_8^{2-}$ with a two- to threefold excess of $CoCl_2$ generates several crystalline colored compounds, of which two have been isolated in pure form by column and plate chromatography (Scheme I). The major product, red diamagnetic **1**, was characterized from its ^{11}B and ^1H FT NMR spectra (Table I), IR (Table II), ^1H FT NMR spectra, and mass spectra as $(Et_4C_4B_8H_8)_2Co_2$ (Figure 1, class 1). A second species, orange paramagnetic **2a**, exhibits no definable NMR spectra and has been characterized from its IR and mass spectra only. The chemical ionization (CI) mass spectrum

(1) Part 12: Maynard, R. B.; Wang, Z.-T.; Sinn, E.; Grimes, R. N. *Inorg. Chem.* **1983**, *22*, 873.
(2) Visiting scholar from the Institute of Chemistry, Academica Sinica, Beijing, China, 1981-1983.
(3) (a) Wade, K. *Adv. Inorg. Chem. Radiochem.* **1976**, *18*, 1. (b) Rudolph, R. W. *Acc. Chem. Res.* **1976**, *9*, 446. (c) Mingos, D. M. P. *Nature (London), Phys. Sci.* **1972**, *236*, 99. (d) O'Neill, M. E.; Wade, K. In "Metal Interactions with Boron Clusters"; Grimes, R. N., Ed.; Plenum Press: New York, 1982; Chapter 1, and references therein.
(4) (a) Grimes, R. N. *Adv. Inorg. Chem. Radiochem.* **1983**, *26*, 55 and references therein. (b) Maxwell, W. M.; Miller, V. R.; Grimes, R. N. *Inorg. Chem.* **1976**, *15*, 1343. (c) Venable, T. L.; Maynard, R. B.; Grimes, R. N. *J. Am. Chem. Soc.* **1984**, *106*, 6187.
(5) Grimes, R. N.; Pipal, J. R.; Sinn, E. *J. Am. Chem. Soc.* **1979**, *101*, 4172.
(6) Wang, Z.-T.; Sinn, E.; Grimes, R. N. *Inorg. Chem.*, following paper in this issue.

0020-1669/85/1324-0826$01.50/0